THE SINH-COSH INTERACTION MODEL

by

Rudolf A. Römer

A dissertation submitted to the faculty of
The University of Utah
in partial fulfillment of the requirements for the degree of

Doctor of Philosophy

Department of Physics

The University of Utah

June 1994

THE UNIVERSITY OF UTAH GRADUATE SCHOOL

SUPERVISORY COMMITTEE APPROVAL

of a dissertation submitted by

Rudolf A. Römer

This dissertation has been read by each member of the following supervisory committee and by majority vote has been found to be satisfactory.

4/27/94.

_____
Chair: Bill Sutherland

4/27/94

_____
Alexei Efros

4/27/94

_____
William Ohlsen

4/27/94

_____
Mikhail Raikh

4/27/94

_____
Yong-Shi Wu

THE UNIVERSITY OF UTAH GRADUATE SCHOOL

FINAL READING APPROVAL

To the Graduate Council of the University of Utah:

I have read the dissertation of _____ Rudolf A. Römer _____ in its final form and have found that (1) its format, citations, and bibliographic style are consistent and acceptable; (2) its illustrative materials including figures, tables, and charts are in place; and (3) the final manuscript is satisfactory to the Supervisory Committee and is ready for submission to The Graduate School.

5/5/94

Date

Bill Sutherland
Chair, Supervisory Committee

Approved for the Major Department

Craig Taylor
Chair/Dean

Approved for the Graduate Council

Ann W. Hart
Dean of The Graduate School

ABSTRACT

We present the exact solution to a one-dimensional, two-component, quantum many-body system in which like particles interact with a pair potential $s(s+1)/\sinh^2(r)$, while unlike particles interact with a pair potential $-s(s+1)/\cosh^2(r)$. We call this the SC model, for the sinh-cosh interaction. After giving a proof of integrability, we then derive the coupled equations determining the complete spectrum. All singularities occur in the ground state when there are equal numbers of the two components; we give explicit results for the ground state and low-lying states in this case. For $s > 0$, the system is an antiferromagnet/insulator, with excitations consisting of a pair–hole–pair continuum, a two-particle continuum with gap, and excitons with gaps. For $-1 < s < 0$, the system has excitations consisting of a hole-particle continuum, and a two-spin wave continuum, both gap-less, and we may be usefully view the SC model as a Heisenberg-Ising fluid with moving Heisenberg-Ising spins. Using finite-size scaling methods of conformal field theory, we calculate the asymptotic expressions and critical exponents for correlation functions of these gapless excitations at zero temperature. The conformal structure is closely related to the Hubbard model with repulsive on-site interaction, although the critical anomaly c can not be read off from the finite-size corrections to the ground state energy. We then investigate the transport properties of the model by threading it with a flux. The Luttinger liquid relation for the stiffness and the susceptibility is derived, both from conformal arguments, and directly from the integral equations. Finally, we investigate the opening and closing of the ground state gaps for both SC and Heisenberg-Ising models, as the interaction strength is varied.

To Yoginie

CONTENTS

LIST OF FIGURES

ACKNOWLEDGMENTS

CHAPTER 1

INTRODUCTION

1.1   Exactly-Soluble Many-Body Systems

Low-dimensional, many-body systems are an important testing ground of theoretical ideas and methods in physics. The restriction of the possible degrees of freedom in these systems, due to their low-dimensionality, reduces some of the analytical and numerical complications in solving them. However, the systems are rich enough in physical structure that it might be that the understanding gained could be generalized to higher dimensions. Furthermore, the recent discoveries of high-T_c superconductivity [1] and quantum Hall effect [2, 3] have renewed interest in these systems in their own right, since the reduced dimensionality seems to be the paramount cause for these effects.

Particles confined to a line can not go around each other and, in this sense, have to interact strongly with each other. However, by looking at the scattering process of two incoming particles, we see that conservation of energy and momentum restricts the scattering to a single outgoing channel. Therefore, there are no dissipative effects such as, e.g., thermalization of the momenta for a two-body scattering. Only scattering processes involving more than two particles can give dissipation. Furthermore, for a system with interaction range ζ, the mean-free-path for a three-body collision is $1/\zeta d^2$ with d the particle density. Thus for ζ sufficiently small — like a δ-function gas — this mean-free-path will be huge. Therefore, we may expect that for an incoming M-body state with amplitude $A(p_1, \ldots, p_M)$, the scattering will be of the two-body type only and simply rearrange the momenta such that the outgoing amplitude is $A(p_{\Pi 1}, \ldots, p_{\Pi M})$. The eigenfunctions can then be written as

$$\Psi(x) \rightarrow \sum_{\Pi} A(\Pi) \exp \left[i \sum_{1 \leq j \leq M} x_j p_{\Pi j} \right], \tag{1.1}$$

and there is no thermalization. This nondiffraction property is at the heart of the Bethe-Ansatz and has been used by Bethe in 1931 to solve the Heisenberg chain [4]. Other models solved by this method are the δ-function gas [5, 6, 7, 8, 9, 10], the Hubbard model

[14] and the anisotropic Heisenberg-Ising chain [11, 12, 13]. Certainly, not all possible interactions will fall into this picture and it has been shown that in order for the Bethe Ansatz to hold, we have a set of consistency equations that imposes restrictions on the set of possible interaction potentials [15, 16]. In general, these nondiffractive potentials are called integrable [17].

The reduced dimensionality also affects the statistical properties of a given system. Particle exchanges in two dimensions may be either clockwise or counterclockwise and in one-dimensions we have a linear ordering of particle positions. Suppose we study a one-component one-dimensional model such that the reflection amplitude is zero. Then the two-body scattering results in a phase shift only. This phase shift is due to (i) the dynamical scattering phase $\theta_d(k - k')$, dependent on the relative momenta and (ii) the statistical phase θ_s. These two phases add up and we may reinterpret the process as a scattering of free particles without dynamical phase but statistical phase shift $\theta \equiv \theta_s + \theta_d(k - k')$. Thus we can see that one-dimensional systems may be viewed as having a statistical interaction only. For θ independent of the momenta, the resulting statistics is known as *fractional* statistics [39]; for θ explicitly a function of k, k', it is called *mutual* statistics [19].

Of special interest in this context is the g/r^2 model which has been solved exactly by Sutherland [20] in 1972 and which is closely related to the important edge states in the quantum Hall effect [21], and also, surprisingly, to level distributions in quantum chaotic systems [22]. In particular, a lattice version of the periodic g/r^2 model, the so-called Haldane-Shastry model [23, 24], has been studied extensively in the last few years. This model has striking similarities to the Heisenberg antiferromagnetic chain, and is intimately linked with Gutzwiller projection of free Fermi states, a useful technique in strongly correlated fermi systems. Also, the algebraic structures in these models are currently under investigation in the context of quantum groups [25].

In this thesis, we will present a study of a model of the g/r^2 type with competing interactions. We have two types of particles and a two-body potential such that like particles repel and unlike particles attract, or vice versa depending on the sign of the interaction strength s. This new model is closely related to the above mentioned systems and we will argue that it may be usefully viewed as a Heisenberg-Ising fluid with moving spins.

After introducing the Hamiltonian in the next section, we then present its solution via

the asymptotic Bethe Ansatz in Chapter 2, where we also show integrability. Ground state properties and excitations in the thermodynamic limit are studied in Chapter 3. For an equal number of particles of the two components, the ground state for $s > 0$ corresponds to an antiferromagnet/insulator. Excitations consist of a gapless pair-hole–pair continuum, a two-particle continuum with gap and excitons with gap. For $-1 < s < 0$, the system has two gapless excitations — a particle-hole continuum and a two spin-wave continuum. In Chapter 4, using finite-size scaling methods of conformal field theory, we calculate the asymptotic expressions and critical exponents for correlation functions of these gapless excitations at zero temperature. The conformal structure is closely related to the Hubbard model with repulsive on-site interaction. However, we can not simply read off the critical anomaly c from the finite-size corrections to the ground state energy. This is also true of the periodic g/r^2 model and we give arguments why this formula may fail. For $-1 < s < 0$ the system behaves very much like a Heisenberg-Ising fluid. We proceed to thread it with a flux Φ in Chapter 5 and study its resulting transport properties. We examine the periodicity of the spectrum as a function of the flux for varying interaction strength and show that — just as for the Heisenberg-Ising chain [13] — there exist threshold values of s where the periodicity becomes macroscopic, i.e., implying free acceleration.

1.2   The SC Model

We present the exact solution to a one-dimensional, two-component, quantum many-body system of considerable complexity. The two kinds of particles are distinguished by a quantum number $\sigma = \pm 1$, which may be thought of as either spin or charge. The system is defined by the Hamiltonian

$$H = -\sum_{1 \leq j \leq N} \frac{1}{2} \frac{\partial^2}{\partial x_j^2} + \sum_{1 \leq j < k \leq N} v_{jk}(x_j - x_k), \tag{1.2}$$

where the pair potential is

$$v_{jk}(x) = s(s+1) \left[\frac{1 + \sigma_j \sigma_k}{2\sinh^2(x)} - \frac{1 - \sigma_j \sigma_k}{2\cosh^2(x)} \right]. \tag{1.3}$$

We assume $s \geq -1$ such that we have a finite bound on the ground state energy [26, Chapter 35]. We call this the SC model, for the sinh-cosh interaction. Thus for $s > 0$, like particles repel, and unlike particles attract. When like particles are near, the repulsive potential increases as $1/r^2$, but for large separations, both potentials decay exponentially with a decay length we take as our length scale, and hence unity. The potentials might usefully be thought of as a screened $1/r^2$ potential.

This system was first introduced by Calogero *et al* [27], who showed it to be integrable. Sutherland [28] soon afterward showed that the system could be exactly solved, and gave the solution for a single component system. He further showed the Toda lattice to be the low-density limit, and was able to take the classical limit to reproduce Toda's celebrated results, identifying the particle-hole excitations of the quantum system with the soliton-phonon modes of the classical system.

Let us begin.

CHAPTER 2

THE ASYMPTOTIC BETHE ANSATZ
SOLUTION

Our solution for the two-component system exploits in a fundamental way the integrability of the system, so we discuss this point first. The two-body problem, which gives us the particle-particle phase shifts, is studied next. We then show that indeed the consistency equations are obeyed and proceed to write the Bethe Ansatz wave function and the Bethe Ansatz equations.

2.1 Integrability

For a classical system of N one-dimensional particles, Lax [30], Moser [31] and Calogero [32] have shown that for certain potentials one can find two Hermitean $N \times N$ matrices L and A that obey the Lax equation $dL/dt = i[A, L]$. Thus L evolves by a unitary transformation generated by A, and hence $\det[L - \omega \mathbb{1}]$ is a constant of motion. Expanding the determinant in powers of ω, we find N integrals of motion, i.e., $\det[L - \omega \mathbb{1}] = \sum_{0 \leq j \leq N} J_j(-\omega)^{N-j}, j = 1, \ldots, N$. Further, these integrals have been shown to be in involution, and thus the system is integrable.

Under a reasonable assumption for the form of the Lax A and L matrices, Calogero has shown that the most general solution to the Lax equations is given in terms of the Jacobi elliptic function $\mathrm{sn}(x|m)$, and by a suitable choice of parameters, our Hamiltonian is included.

Calogero has also demonstrated that if one replaces the classical dynamical variables with the corresponding quantum mechanical operators, $\det[L - \omega \mathbb{1}]$ is well defined with no ordering ambiguity, and the quantum mechanical commutator $[\![H, \det[L - \omega \mathbb{1}]]\!] = 0$. Thus, the J_j are still constants of motion. Finally, Calogero showed that $[\![\det[L - \omega \mathbb{1}], \det[L - \omega' \mathbb{1}]]\!] = 0$, and thus the quantum system is also completely integrable.

To sum up the situation: Our system is completely integrable. For the general classical system integrability tells us something concrete, namely that the motion in

terms of action-angle variables is on a torus. However, for the general quantum system integrability seems to buy one almost nothing. The exception is for those special cases that support scattering; i.e., systems that fly apart when the walls of the box are removed. In these cases, in the distant past and future the Lax matrix L approaches a diagonal matrix with the momenta as diagonal elements, so that $\det[L - \omega \mathbb{1}] = \prod_{1 \leq j \leq N}(p_j - \omega)$. Thus the individual momenta p_j are conserved in a collision, and hence, as emphasized by Sutherland [28, 29], the wavefunction is given asymptotically by Bethe's Ansatz. Sutherland has exploited this fact to completely determine, in the thermodynamic limit, properties of systems interacting by such potentials including our system. We stress that no features of the proof of integrability are needed. All we need is to know it to be integrable, by whatever method.

The proof of Calogero, however, is very difficult, and only briefly sketched in the literature. For that reason, we now offer an alternative proof of integrability based on a method of Shastry [33]. Let us write the Lax matrices as

$$A_{jk} = \delta_{jk}\sum_{l \neq j}\alpha'_{jl} + (\delta_{jk} - 1)\alpha'_{jl}, \tag{2.1}$$

$$L_{jk} = \delta_{jk}p_j + i(1 - \delta_{jk})\alpha_{jk}, \tag{2.2}$$

where

$$\alpha_{jk} = -s\left[\frac{1 + \sigma_j\sigma_k}{2}\coth(x_j - x_k) + \frac{1 - \sigma_j\sigma_k}{2}\tanh(x_j - x_k)\right]. \tag{2.3}$$

Then if the two-body potential potential v_{jk} is given by $v_{jk} = \alpha_{jk}^2 + \alpha'_{jk} - s^2$, we find that the quantum Lax equation $[\![H, L]\!] = [L, A]$ is satisfied. Here the first fancy commutator is a quantum mechanical commutator between operators, whereas the second commutator is an ordered matrix commutator, so that the equation above is really N^2 equations of the form $[H, L_{jk}] = \sum_{1 \leq l \leq N}(L_{jl}A_{lk} - A_{jl}L_{lk})$. This potential, however, is exactly the potential for our system.

We now observe that the Lax A matrix has the following very important property. Defining a vector ζ with $\zeta_j = 1$, we see $A\zeta = \zeta^\dagger A = 0$. This allows us to construct constants of motion by $I_n = \zeta^\dagger L^n \zeta$, since

$$[\![H, I_n]\!] = \zeta^\dagger [\![H, L^n]\!]\zeta \tag{2.4}$$

$$= \zeta^\dagger \sum_{0 < j < n-1}\left\{L^j[\![H, L]\!]L^{n-1-j}\right\}\zeta \tag{2.5}$$

$$= \zeta^\dagger \sum_{0 < j < n-1}\left\{L^j[A, L]L^{n-1-j}\right\}\zeta \tag{2.6}$$

$$= \zeta^{\dagger} \left\{ A L^{n-1} - L^{n-1} A \right\} \zeta = 0. \tag{2.7}$$

By Jacobi's relation for commutators, $[\![I_n, I_m]\!]$ is a constant of motion, and since this is a system that supports scattering, we see $[\![I_n, I_m]\!] \to 0$, and hence the system is completely integrable.

2.2 The Two-Body Problem

Having shown the system to be integrable, we then know that the model has a complete set of conserved quantities and that any many-body scattering event is just a sequence of two-body scatterings. Therefore the set of momenta for an incoming state will be simply rearranged by the scattering event, and so the wavefunction has to be of the Bethe Ansatz form at least asymptotically. Then the only further input needed for the Bethe Ansatz is the solution to the two-body problem. For a system that supports scattering and which has a convergent virial series, this asymptotic form of the wave function is enough to insure that our results will become *exact* in the thermodynamic limit, i.e., $L \to \infty$ at fixed density [17].

First, we discuss like particles. In terms of the relative coordinate $r = x_2 - x_1$, the potential is $s(s+1)/\sinh^2(r)$ and the relative momentum $k = (k_2 - k_1)/2$. The center-of-mass motion factors and we now seek a solution to the equation

$$\phi''(r) + \left[k^2 - \frac{s(s+1)}{\sinh^2(r)} \right] \phi = 0, \tag{2.8}$$

such that asymptotically,

$$\phi(r) \sim \left\{ \begin{array}{ll} r^{s+1} & r \to 0+, \\ e^{-ikr} + S(2k)e^{ikr} & r \to +\infty. \end{array} \right. \tag{2.9}$$

Let us make a change of variables, i.e.,

$$\phi(r) = [\sinh(r)]^{-ik} y(u(r)), \tag{2.10}$$

$$u(r) = 1/(1 - e^{2r}). \tag{2.11}$$

The equation for $y(u)$ now reads as

$$u(1-u)y''(u) + (ik+1)(1-2u)y'(u) - (ik-s)(ik+s+1)y(u) = 0. \tag{2.12}$$

This second order differential equation is solved by hypergeometric functions $F(\alpha, \beta, \gamma, x)$. Choosing $\alpha = ik+s+1$, $\beta = ik-s$ and $\gamma = ik+1$, then $y_1(u) \equiv F(\alpha, \beta, \gamma, u)$ is a solution.

The second independent solution may be written as $y_2(u) \equiv (-u)^{1-\gamma} F(\alpha', \beta', \gamma', u)$ with $\alpha' = \beta - \gamma + 1 = -s$, $\beta' = \alpha - \gamma + 1 = 1 + s$ and $\gamma' = 2 - \gamma = 1 - ik$. However, neither of these solutions is finite at $u \to \infty$, as we can see by an asymptotic expansion [34, 15.3.7].

$$
\begin{aligned}
F(\alpha, \beta, \gamma, u) \\
= \quad & \frac{\Gamma(\gamma)\Gamma(\beta - \alpha)}{\Gamma(\beta)\Gamma(\gamma - \alpha)} (-u)^{-\alpha} F(\alpha, 1 - \gamma + \alpha, 1 - \beta + \alpha, 1/u) \\
& + \frac{\Gamma(\gamma)\Gamma(\alpha - \beta)}{\Gamma(\alpha)\Gamma(\gamma - \beta)} (-u)^{-\beta} F(\beta, 1 - \gamma + \beta, 1 - \alpha + \beta, 1/u) \\
\overset{u \to \infty}{=} \quad & \frac{\Gamma(\gamma)\Gamma(\beta - \alpha)}{\Gamma(\beta)\Gamma(\gamma - \alpha)} (-u)^{-\alpha} \cdot 1 + \frac{\Gamma(\gamma)\Gamma(\alpha - \beta)}{\Gamma(\alpha)\Gamma(\gamma - \beta)} (-u)^{-\beta} \cdot 1.
\end{aligned}
$$

Thus, the linear combination

$$
y(u) = \frac{\Gamma(\gamma')\Gamma(\beta' - \alpha')}{\Gamma(\beta')\Gamma(\gamma' - \alpha')} y_1(u) - \frac{\Gamma(\gamma)\Gamma(\alpha - \beta)}{\Gamma(\alpha)\Gamma(\gamma - \beta)} y_2(u) \tag{2.13}
$$

is finite as $u \to \infty$. We then determine the phase shift $S(k)$, by looking at the behavior of $y(u)$ as $u \to 0^-$ ($r \to +\infty$),

$$
y(u \to 0^-) = \underbrace{\frac{\Gamma(1 - ik)\Gamma(1 + 2s)}{\Gamma(1 + s)\Gamma(1 + s - ik)}}_{A} \cdot 1 - \underbrace{\frac{\Gamma(1 + ik)\Gamma(1 + 2s)}{\Gamma(1s + ik)\Gamma(1 + s)}}_{B} (-u)^{-ik}. \tag{2.14}
$$

Let us relate this result to the original wave function $\phi(r)$,

$$
\phi(r) \overset{(2.10)}{=} [\sinh(r)]^{-ik} y(u(r)) \tag{2.15}
$$

$$
\overset{r \to \pm\infty}{=} \left[\frac{1}{2}(e^r - e^{-r})\right]^{-ik} \left[A - B\left(\frac{-1}{1 - e^{2r}}\right)^{-ik}\right] \tag{2.16}
$$

$$
\simeq 2^{ik} A \left[e^{-ikr} - (B/A)e^{ikr}\right]. \tag{2.17}
$$

Therefore, the scattering amplitude $S(k)$ is given by

$$
S(k) = -\frac{\Gamma(1 + ik/2)\Gamma(1 + s - ik/2)}{\Gamma(1 - ik/2)\Gamma(1 + s + ik/2)}. \tag{2.18}
$$

This scattering does not rearrange the particles. For bosons (fermions) the wavefunction must be (anti)symmetric, so the scattering amplitude for transmission will be $\pm S(k)$. In this chapter, we will drop factors of -1 in the scattering amplitudes, assuming that they are taken care of by either the choice of statistics of the particles, the choice of quantum numbers as half-odd-integers, or the choice of number of particles as even or odd. We will, however, elaborate on this in the next chapters.

Now, we discuss unlike particles, with the potential $-s(s+1)/\cosh^2(r)$. We need not require $\phi(r=0) = 0$, and so unlike particles may pass through each other. The wave function in the center of mass is then given asymptotically as

$$\phi(r) = \begin{cases} e^{ikr} + R(2k)e^{-ikr} & r \to -\infty, \\ T(2k)e^{ikr} & r \to +\infty. \end{cases} \qquad (2.19)$$

As before, we may write the solution in terms of hypergeometric functions. The explicit calculations are much as before and can be found also in [26, Chapter 18]. The reflection and transmission amplitudes are given as $R(k) = S(k)r(k)$, $T(k) = S(k)t(k)$, where

$$r(k) = \frac{\sin \pi s}{\sin \pi(s + ik/2)}, \qquad (2.20)$$

$$t(k) = -\frac{\sin \pi ik/2}{\sin \pi(s + ik/2)}. \qquad (2.21)$$

Also present are bound states, labeled by an index $m = 1, 2, \ldots, M$, according to increasing energy. Thus the parity of the states is $(-1)^{m-1}$, and even parity states have spin 0, while odd parity states have spin 1. Bound states appear as poles of the reflection and transmission amplitudes, $R(k_1 - k_2)$ and $T(k_1 - k_2)$ on the positive half of the imaginary axis, given by $k_{1,2} = k \pm i\kappa, k > 0$. The momentum and energy of such a bound state is $P = 2k$, and $E = k^2 - \kappa^2$. Let us concentrate on $T(k)$. From [34, 6.1.2], we know that we can rewrite the Γ function as

$$\Gamma(z) = \lim_{n \to \infty} \frac{n! \, n^z}{z(z+1) \cdots (z+n)}, \qquad (2.22)$$

and for $k = i\kappa$,

$$S(i\kappa) = \prod_{l=0}^{\infty} \frac{(l + \kappa)(s + l + 1 - \kappa)}{(l - \kappa)(s + l + 1 + \kappa)}. \qquad (2.23)$$

Thus, for $l = 1, 2, \ldots$, the poles are located at $\kappa = l, -s - l - 1$ and the zeros at $\kappa = -l, s + l + 1$. Furthermore,

$$t(i\kappa) = \prod_{l=-\infty}^{\infty} \frac{l - \kappa}{l + s - \kappa}, \qquad (2.24)$$

such that for $l = 0, \pm 1, \pm 2, \ldots$, the poles lie at $\kappa = l + s$ and the zeros at $\kappa = l$. In the same way, we treat the poles of $r(k)$ and putting it all together, we find $\kappa_m = s + 1 - m$, where $m = 1, 2, \ldots, M$, and $M(s)$ is the largest integer less than s. There are no bound states for $0 \leq s \leq -1$. Threshold values of s are $s = 0, 1, 2, \ldots$, and at these values, the reflection amplitude vanishes. At the bound state poles we also find $r(2i\kappa_m)/t(2i\kappa_m) = (-1)^{m-1}$. We call the bound states *pairs*.

2.3 Consistency and Phase Shifts

2.3.1 Yang-Baxter equations

We know the Yang-Baxter equations [15, 16] must hold, and we can verify this explicitly. For a two-component system the Yang-Baxter equations are equivalent to

$$r_2 = r_3r_1 + t_3r_2t_1 \quad \text{and} \quad r_3t_2 = r_3t_1 + t_3r_2r_1, \tag{2.25}$$

where $r_1 = r(k_1 - k_2), r_2 = r(k_1 - k_3), r_3 = r(k_2 - k_3)$ etc. for t_j. A degenerate situation occurs at a pole in r_3 and t_3, when $k_2 - k_3 = 2i\kappa_m$. There, since $r_3/t_3 = (-1)^{m-1}$, the equations become

$$0 = r_1 + (-1)^{m-1}r_2t_1 \quad \text{and} \quad t_2 = t_1 + (-1)^{m-1}r_2r_1, \tag{2.26}$$

where $r_{2,1} = r(k \pm i\kappa_m)$, and etc. for t_j. These relationships will be important when we calculate phase shifts.

2.3.2 Derivation of various phase shifts

If a particle of type m passes through a particle of type m', without reflection, then we have a scattering amplitude $\exp[-i\theta_{mm'}(k_1 - k_2)]$, and a corresponding phase shift $\theta_{mm'}(k)$. These phase shifts are at the heart of the Bethe Ansatz. Let us label the unbound particle by $m = 0$. Then we have found

$$\theta_{00}(k) = i\log\left[\frac{\Gamma(1 + ik/2)\Gamma(1 + s - ik/2)}{\Gamma(1 - ik/2)\Gamma(1 + s + ik/2)}\right]. \tag{2.27}$$

As we explained, we will not include factors of -1 in the scattering amplitudes, so $\theta_{00}(0) = 0$. In general $\theta_{mm'}(k) = -\theta_{mm'}(-k) = \theta_{m'm}(k)$, and we will find that we always have $\theta_{mm'}(0) = 0$. In Figure (2.1), we plot $\theta_{0,0}(k)$ for various values of the interaction strength s.

Now, consider the scattering of a particle k_1 on a pair of two particles with momenta $k_2 \pm i\kappa_m$. Let $k = k_1 - k_2$. Figure (2.2) depicts the incoming state and in Figure (2.3) we show all three possible outgoing states. There are five possible scattering channels leading to these out states. They are shown in Figure (2.4). Let us briefly describe channel (a), the other four channels should then be self-explanatory: The incoming particle first scatters off a like particle with phase shift $S_1 = S(k - i\kappa_m)$. Then the phase shifted particle encounters an unlike particle and passes through with transmission amplitude
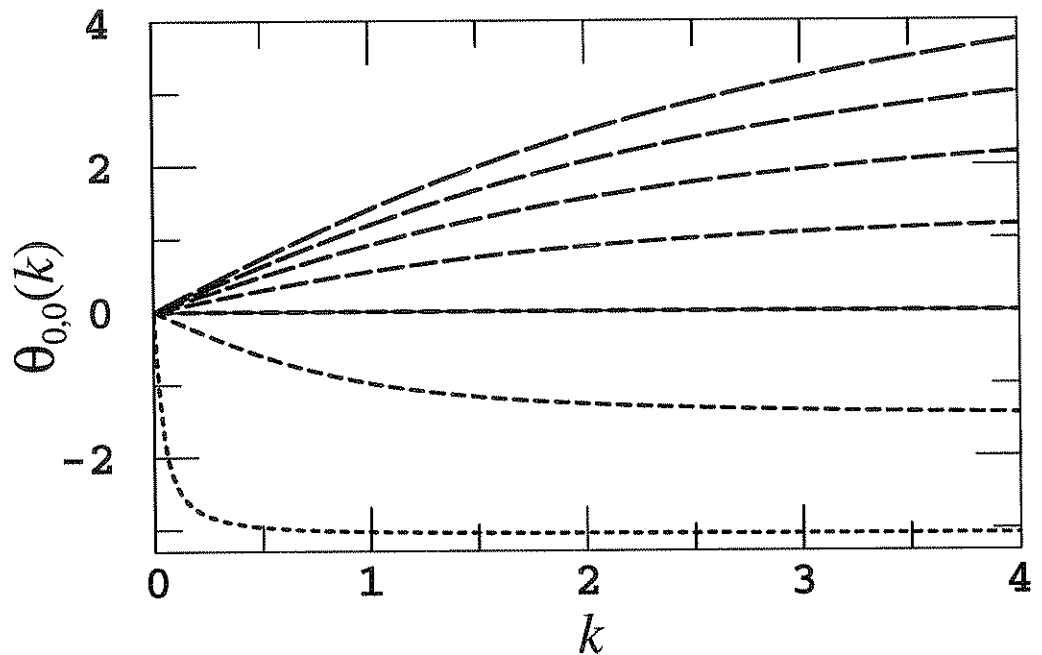
Figure 2.1. Particle-particle phase shift $\theta_{0,0}(k)$ for various values of the interaction strength $s = -0.98, -0.49, 0, 0.49, 0.98, 1.47$, and 1.98, corresponding to increasing dash length.

$$+(-1)^{m-1}$$
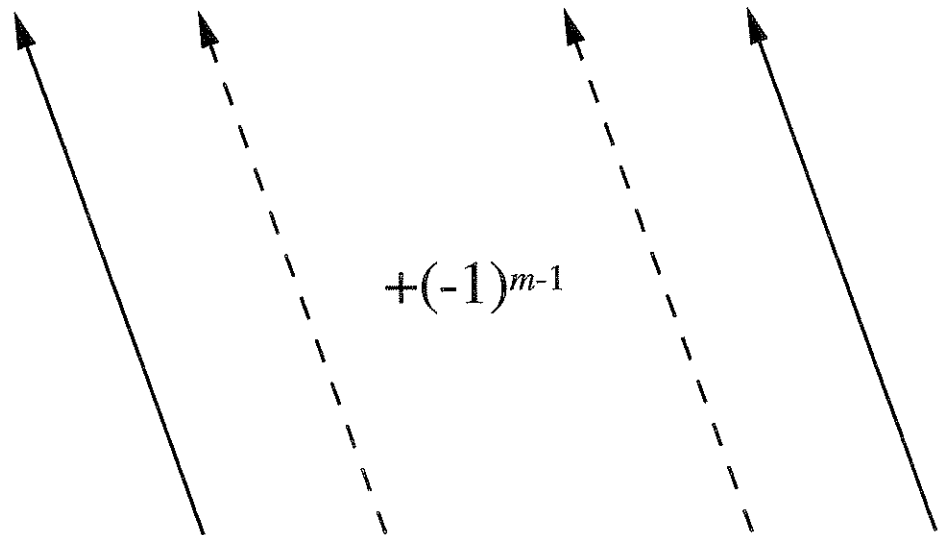
Figure 2.2. A pair of type m. Solid and dashed arrows indicate the two different kinds of particles.
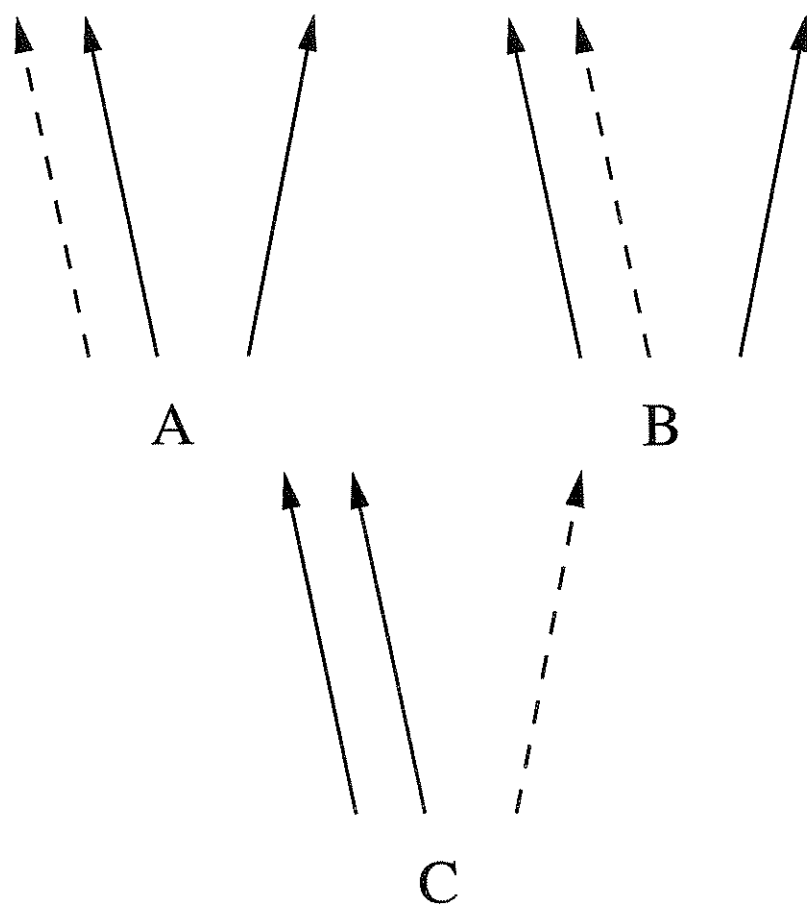
Figure 2.3. The three possible outgoing states for a particle-pair scattering process.
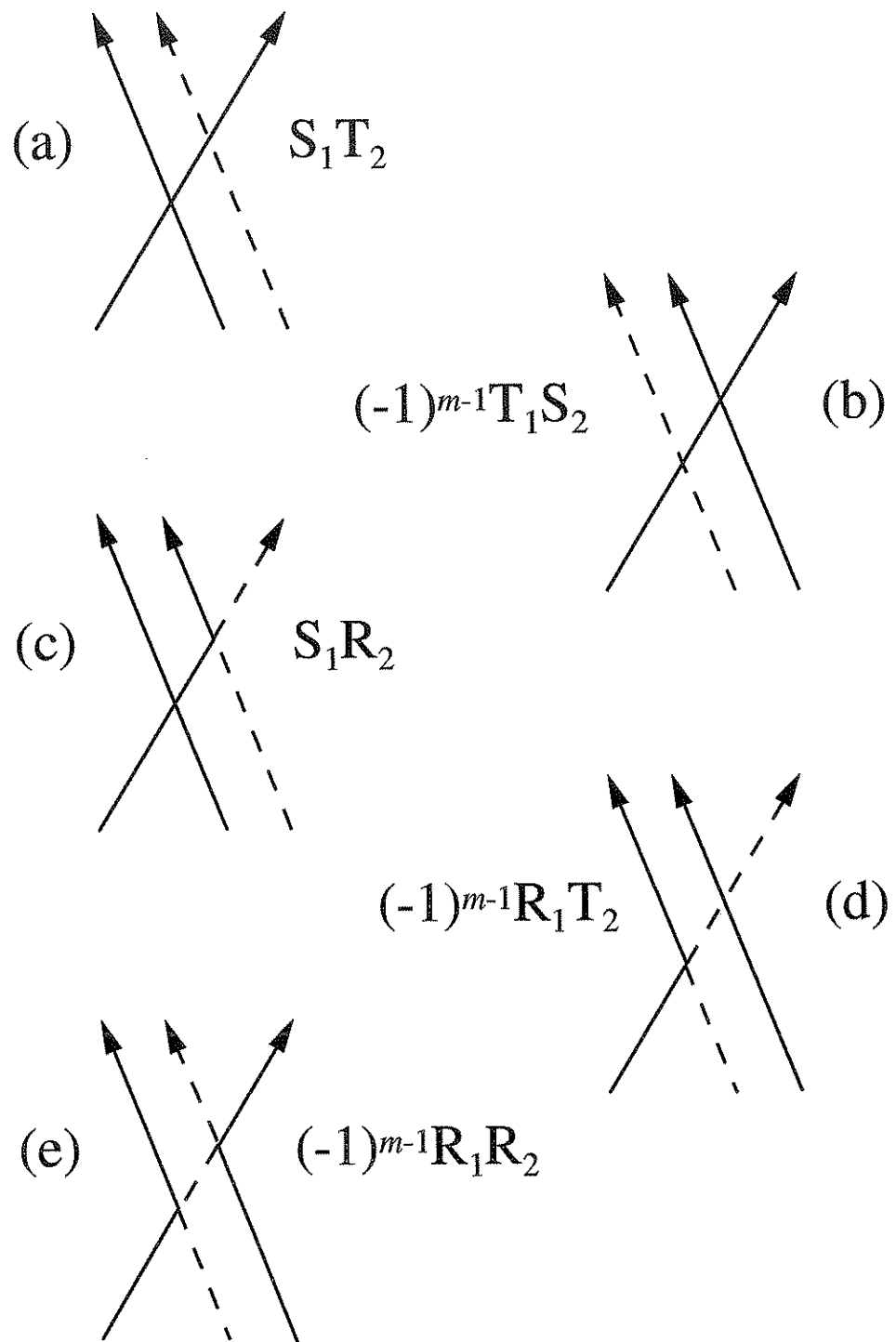
Figure 2.4. Particle-pair scattering channels and their amplitudes as explained in the text.

$T_2 = T(k + i\kappa_m)$. The overall effect of this process should be a net phase shift θ_{0m}, i.e., nondiffractive scattering. Thus we have a set of consistency equations

$$0 \;=\; S_1 S_2 [t_2 - t_1 + (-1)^{m-1} r_1 r_2], \tag{2.28}$$

$$0 \;=\; S_1 S_2 [r_2 + (-1)^{m-1} r_1 t_2]. \tag{2.29}$$

These equations may be proved using the degenerate Yang-Baxter equations (2.26). Thus, we find for the particle-pair scattering amplitude

$$T_1 S_2 \;=\; S(k + i\kappa_m) S(k - i\kappa_m) t(k + i\kappa_m) \equiv \exp[-i\theta_{0m}(k)]. \tag{2.30}$$

Using the explicit forms, we can furthermore verify that $\theta_{0m}(k)$ is real for k real. Figure (2.5) shows the phase shift $\theta_{0,1}(k)$ of particles scattering on pairs of type 1.

Finally, we view the scattering of a pair from a pair as the scattering of two particles with momenta $k_1 \pm i\kappa_m$ from a pair with $k_2 \pm i\kappa_{m'}$ as shown in Figure (2.6). This gives us a net phase shift $\theta_{mm'}(k) = \theta_{0m'}(k - i\kappa_m) + \theta_{0m'}(k + i\kappa_m)$. Again, using the explicit forms, we can verify that $\theta_{mm'}(k)$ is real for k real, and symmetric in m, m'. In Figure (2.7), we plot the resulting phase shift of type 1 pairs. Furthermore, in Figure (2.8), we
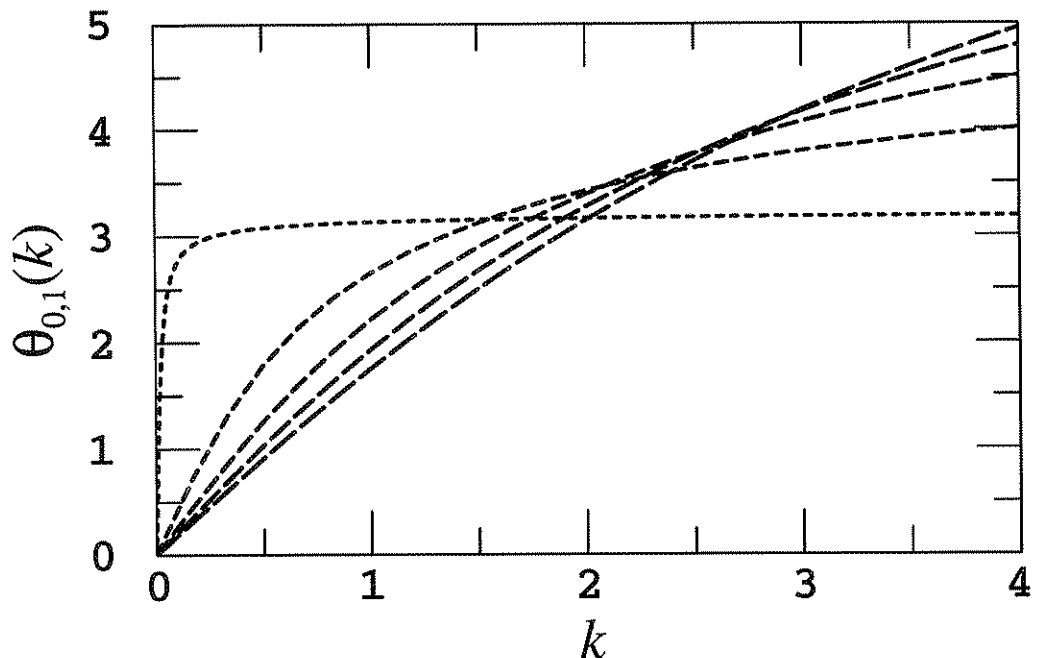
Figure 2.5. Particle-pair phase shift $\theta_{0,1}(k)$ for various values of the interaction strength $s = 0.02, 0.51, 1.00, 1.49, 1.98$, corresponding to increasing dash length.

Figure 2.6. A pair-pair scattering process consists of two subsequent particle-pair scattering processes.
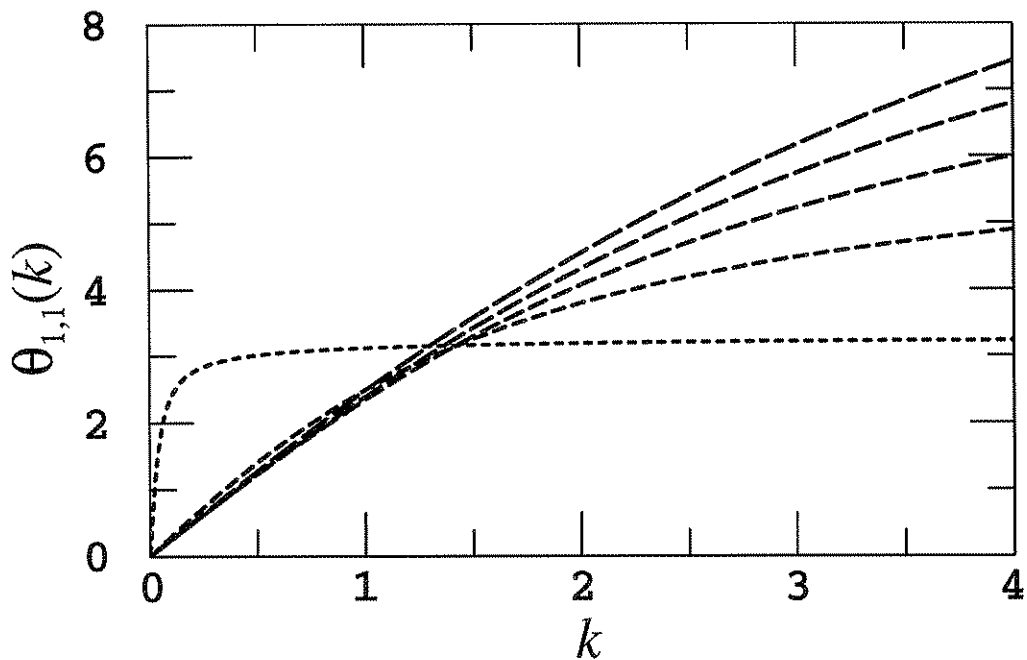
Figure 2.7. Pair-pair phase shift $\theta_{1,1}(k)$ for various values of the interaction strength $s = 0.02, 0.51, 1.00, 1.49, 1.98$, corresponding to increasing dash length.
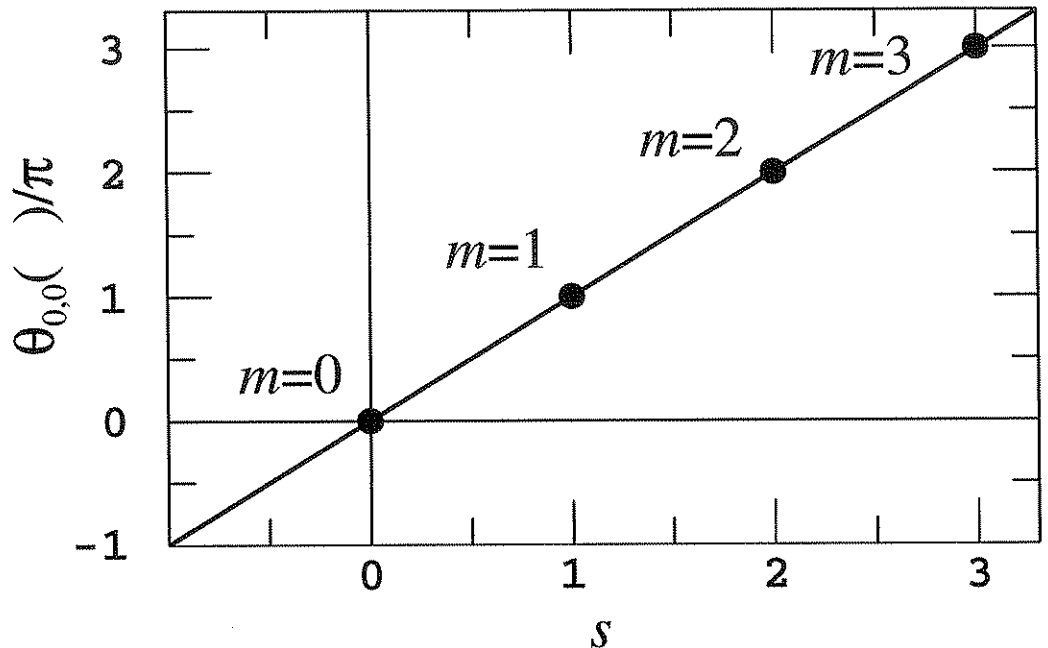
Figure 2.8. At the threshold values for a new bound state, i.e., s = integer, we have $\theta_{0,0}(\infty)/\pi$ = number of bound states.

show $\theta_{11}(\infty)$ as a function of s and the graph is very much reminiscent of Levinson's theorem, i.e.,

$$\theta_{0,0}(\infty)/\pi = \text{number of bound states.} \qquad (2.31)$$

To summarize: We have $N_\uparrow$ particles with $\sigma = +1$, and $N_\downarrow$ with $\sigma = -1$, for a total of $N = N_\uparrow + N_\downarrow$. Let us assume $N_\uparrow \geq N_\downarrow$. Further, pairs of up-down spins bind into a variety of bound states, or pairs, labeled by m, $m = 1, \ldots, M(s)$. Let there be N_m of each type. Then the number of unbound particles is $N_0 = N - 2 \sum_{1 \leq m \leq M} N_m$. We will call these simply particles from now on. They would correspond to *spinons/ions* in the spin/charge picture. Of these particles, we have N_{-1} with spin down; let us call them *spin waves*. Clearly $N_{-1} = N_\downarrow - \sum_{1 \leq m \leq M} N_m$, and $N_{-1} \leq N_0/2$.

We still must treat the dynamics of the spin waves, but since they are not "real" particles, but only correlations in the quantum numbers of particles, they have no momentum or energy directly. Thus, we define

$$\eta_m = \begin{cases} 0, & m = -1, \\ 1, & m = 0, \\ 2, & m = 1, 2, \ldots, M(s); \end{cases} \qquad (2.32)$$

then we can write the momentum and energy as

$$P = \sum_{-1 \leq m \leq M} \eta_m \sum_{k_m} k_m, \tag{2.33}$$

$$E = \frac{1}{2} \sum_{-1 \leq m \leq M} \eta_m \sum_{k_m} k_m^2 - \sum_{1 \leq m \leq M} N_m \kappa_m^2. \tag{2.34}$$

2.4 Bethe-Ansatz Equations

Since particle-pair and pair-pair pass through one another with only a phase shift and no reflection, their interaction is in some sense trivial. However, particles do scatter from particles with reflection, and their interaction is not trivial. We write the asymptotic wavefunction explicitly in the Bethe Ansatz form, and for now consider only the N_0 particles. We use the spin language, so $\sigma_z(j) = \pm 1$ according to whether the jth particle in the ordering $x_1 < ... < x_{N_0}$ has spin up or down. A choice for all $\sigma_z(j)$ we denote simply by σ. Then asymptotically the wave function is given by

$$\Psi(x|\sigma) \to \sum_{\Pi} A(\Pi|\sigma) \exp \left[i \sum_{1 \leq j \leq N_0} x_j k_{\Pi j} \right]. \tag{2.35}$$

The summation is over all the $N_0!$ permutations of the momenta. We arrange the $A(\Pi|\sigma)$ for fixed Π as a column vector $\xi(\Pi)$. Then the Yang-Baxter equations ensure that we can find a consistent set of amplitudes $A(\Pi|\sigma)$, by finding the simultaneous eigenvector of the N_0 equations

$$e^{ik_j L} \prod_{1 \leq n \leq N_0} S(k_j - k_n) X_{j,j-1} \cdots X_{j,1} X_{j,N_0} \cdots X_{j,j+1} \xi(I) = \xi(I). \tag{2.36}$$

In this equation, the $X_{j,n}$ are operators given as

$$
\begin{aligned}
X_{j,n} &= \frac{1 + t(k)}{2} \mathbb{1} + \frac{1 - t(k)}{2} \sigma_z(j) \sigma_z(n) \\
&\quad + \frac{r(k)}{2} \left[\sigma_x(j) \sigma_x(n) + \sigma_y(j) \sigma_y(n) \right],
\end{aligned} \tag{2.37}
$$

where $k = k_{\Pi j} - k_{\Pi n}$.

These eigenvalue equations can in turn be solved by a Bethe Ansatz for the N_{-1} overturned spins — the spin waves — on a lattice of N_0 particles. These equations can be solved either: (i) directly, by the methods of Yang [35]; (ii) with commuting transfer matrices, by the methods of Baxter [36]; or (iii) by quantum inverse scattering methods of Faddeev and Takhtajan [37]. We are not aware that these equations have appeared

before in the solution of a quantum many-body problem, although the low-density case has often appeared, for instance first in Yang's original solution for δ-function fermions.

The solution is sufficiently technical as to be rather unpleasant to spell out. Moreover, a general solution for a two-component model, given in terms of $t(k)$ and $r(k)$, has been given already in [38] and thus we refrain from repeating it here. Using those formulas, we find for the eigenvalues of the previous equations,

$$e^{ik_j L} \prod_{1 \leq n \leq N_0} S(k_j - k_n) \prod_{1 \leq q \leq N_{-1}} \frac{\sin \pi[s - i(k_j - \lambda_q)]/2}{\sin \pi[s + i(k_j - \lambda_q)]/2} = 1. \qquad (2.38)$$

In this equation, the λ's are the momenta of the spin waves, and are determined from the equation

$$\prod_{1 \leq q \leq N_{-1}} \frac{\sin \pi[s + i(\lambda_j - \lambda_q)/2]}{\sin \pi[s - i(\lambda_j - \lambda_q)/2]} \prod_{1 \leq n \leq N_0} \frac{\sin \pi[s - i(\lambda_j - k_n)]/2}{\sin \pi[s + i(\lambda_j - k_n)]/2} = 1. \qquad (2.39)$$

We now have our two final phase shifts, for particle-spin wave and spin wave-spin wave scattering:

$$\theta_{0,-1}(k) = i \log \left[\frac{\sin \pi[s - ik]/2}{\sin \pi[s + ik]/2} \right], \qquad (2.40)$$

$$\theta_{-1,-1}(k) = i \log \left[\frac{\sin \pi[s + ik/2]}{\sin \pi[s - ik/2]} \right]. \qquad (2.41)$$

As noted, there is no phase shift for spin wave-pair scattering. In Figures (2.9) and (2.10), we plot these phase shifts for varying s. At the threshold values $s =$ integer, the spin wave modes uncouple completely from the particles, and thus from the system, since they contribute no energy or momentum directly. In this case, we have the very high degeneracies found in the $1/r^2$ lattice systems [39, 40], and for the same reason — an absence of reflection.

Let us now impose periodic boundary conditions and take any particle, pair or spin wave with momentum $P = \eta k$ around a ring of large circumference. Along the way, it suffers a phase change as it scatters from every other particle, pair or spin wave, plus a phase change of PL. Periodicity requires that this phase change be an integer multiple of 2π, the integer being the quantum number. We write this statement as coupled equations in a rather symbolic form:

$$L\eta_m k_m = 2\pi I_m(k_m) + \sum_{-1 \leq m' \leq M} \sum_{k'_{m'}} \theta_{m,m'}(k_m - k_{m'}), \quad m = -1, 0, 1, \ldots, M. \qquad (2.42)$$

Here the $I_m(k_m)$ are the quantum numbers, the only subtlety being that for the spin waves, I_{-1} ranges only over $1, \ldots, N_0$.
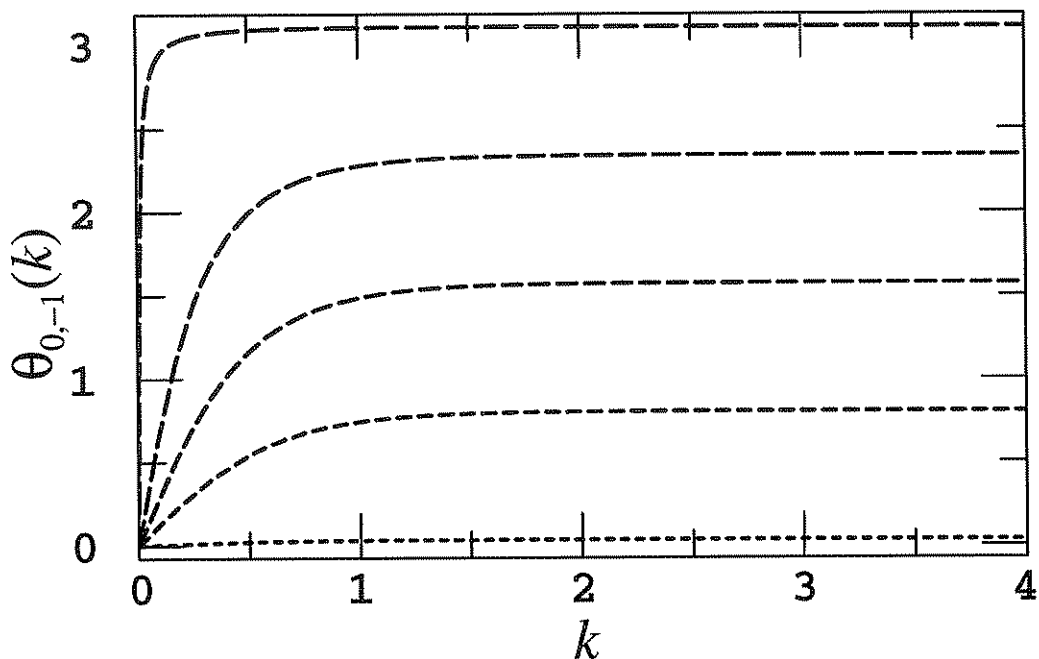
Figure 2.9. Particle-spin wave phase shift $\theta_{0,-1}(k)$ for various values of the interaction strength $s = -0.99, -0.75, -0.50, -0.25, -0.01$, corresponding to increasing dash length.
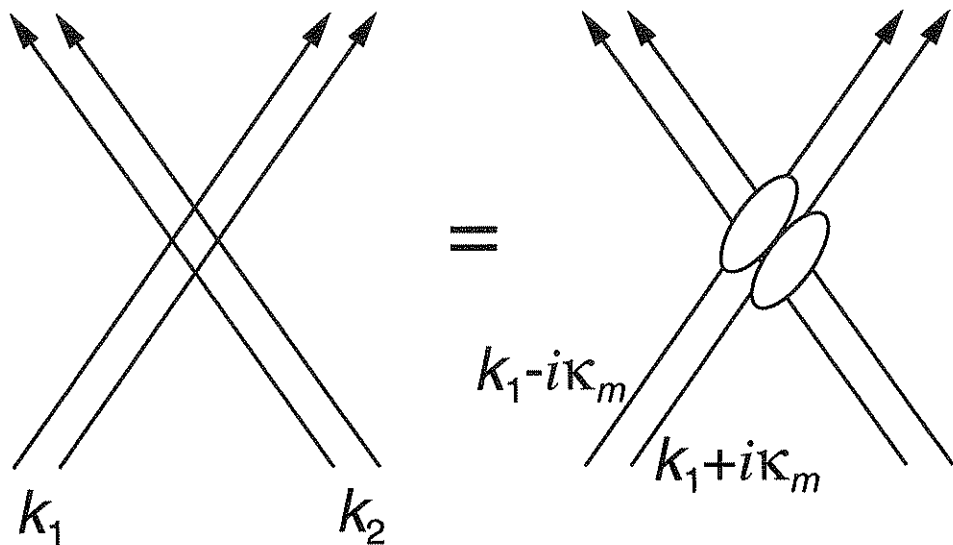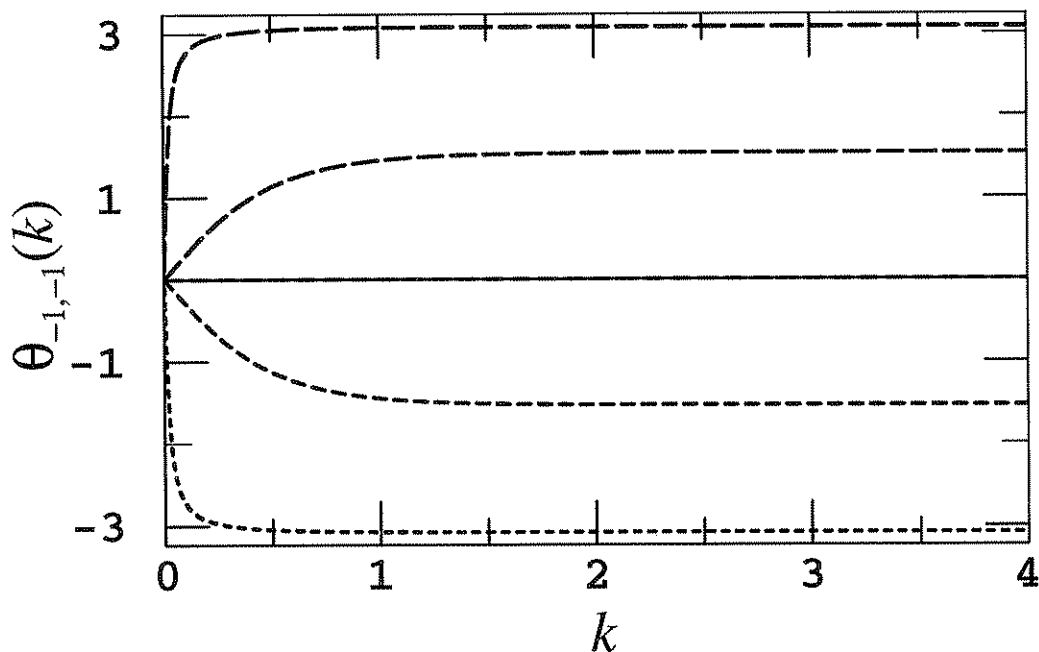

Figure 2.10. Spin wave-spin wave phase shift $\theta_{-1,-1}(k)$ for various values of the interaction strength $s = -0.99, -0.75, -0.50, -0.25, -0.01$, corresponding to increasing dash length.

CHAPTER 3

PROPERTIES OF LOW-LYING STATES

In this chapter, we give explicit results for the ground state and (other) low-lying states when $N_\uparrow = N_\downarrow$, which we call the *spin/charge zero-sector*. This certainly is the most interesting case, since all singularities in the $(N_\uparrow, N_\downarrow)$ ground state phase diagram occur for $N_\uparrow = N_\downarrow$. In fact, as we shall see, for $s > 0$, the chemical potential has a discontinuity across the line $N_\uparrow = N_\downarrow$, and thus the system is an antiferromagnet/insulator, although not of the Neel/Mott type. For $-1 < s < 0$, there is a weak singularity at $N_\uparrow = N_\downarrow$, without a discontinuity in the chemical potential.

3.1 The Unbound Case

3.1.1 The Ground State

For $-1 < s < 0$, there are no bound states and we will call this the *unbound case* in the sequel. From Equation (2.42), we therefore have only two coupled equations for N_0 particles with pseudo-momenta $\mathbf{k}_0 = (k_1, \ldots, k_{N_0})$ and N_{-1} spin waves with rapidities $\mathbf{k}_{-1} = (\lambda_1, \ldots, \lambda_{N_{-1}})$.

$$Lk_j = 2\pi I_j(k_j) + \sum_{\alpha=1}^{N_{-1}} \theta_{0,-1}(k_j - \lambda_\alpha) + \sum_{l=1}^{N_0} \theta_{0,0}(k_j - k_l), \quad (3.1a)$$

$$0 = 2\pi J_\alpha(\lambda_\alpha) + \sum_{\beta=1}^{N_{-1}} \theta_{-1,-1}(\lambda_\alpha - \lambda_\beta) + \sum_{j=1}^{N_0} \theta_{-1,0}(\lambda_\alpha - k_j). \quad (3.1b)$$

In the thermodynamic limit, i.e., $L \to \infty$ with fixed $d_0 \equiv N_0/L$, $d_{-1} \equiv N_{-1}/L$, the ground state is a filled Fermi sea characterized by the distribution function $\rho(k)$ of particles and $\sigma(\lambda)$ of down-spins.

$$\rho(k) = \frac{1}{2\pi} - \frac{1}{2\pi} \int_{-C}^{C} \theta'_{0,-1}(k - \mu)\sigma(\mu)d\mu - \frac{1}{2\pi} \int_{-B}^{B} \theta'_{0,0}(k - h)\rho(h)dh, \quad (3.2a)$$

$$\sigma(\lambda) = 0 - \frac{1}{2\pi} \int_{-C}^{C} \theta'_{-1,-1}(\lambda - \mu)\sigma(\mu)d\mu - \frac{1}{2\pi} \int_{-B}^{B} \theta'_{-1,0}(\lambda - h)\rho(h)dh. \quad (3.2b)$$

Here the prime denotes the first derivative. The values of B and C are fixed by the following equations:

$$\int_{-B}^{B} \rho(k)\mathrm{d}k \;\; = \;\; d_0, \tag{3.3a}$$

$$\int_{-C}^{C} \sigma(\lambda)\mathrm{d}\lambda \;\; = \;\; d_{-1} = d_0/2 - \mathcal{M}, \tag{3.3b}$$

where $\mathcal{M} = (N_\uparrow - N_\downarrow)/2L$ is the magnetization per unit length.

Let us now restrict our discussion to the zero sector, when $N_0 = N$, $N_{-1} = N/2$ and $\mathcal{M} = 0$. Since $\sigma(\lambda) \geq 0$, this corresponds to the limit C of the spin wave distribution integration being ∞. Following [13], we introduce an operator notation, i.e., $\langle k|\rho\rangle \equiv \rho(k)$, $\langle \lambda|\sigma\rangle \equiv \sigma(\lambda)$ and $\langle k|K_{m,m'}|h\rangle \equiv \frac{1}{2\pi}\theta'_{m,m'}(k-h)$. Furthermore, B and C are defined as projection operators to yield the finite limits of integration, i.e.,

$$B\rho = \left\{ \begin{array}{ll} \rho(k) & \text{for } -B \leq k \leq B, \\ 0 & \text{for } |k| \geq B. \end{array} \right. \tag{3.4}$$

Then for zero magnetization, the ground state equations may be written as

$$\rho + K_{0,0}B\rho + K_{0,-1}\sigma \;\; = \;\; \zeta, \tag{3.5a}$$

$$\sigma + K_{-1,-1}\sigma + K_{0,-1}B\rho \;\; = \;\; 0. \tag{3.5b}$$

We introduce the resolvent $J_{-1,-1}$ such that $(1 + J_{-1,-1})(1 + K_{-1,-1}) = (1 + K_{-1,-1})(1 + J_{-1,-1}) = \mathbb{1}$. Then $\sigma = -(1 + J_{-1,-1})K_{0,-1}B\rho$ and

$$\zeta = \rho + [K_{0,0} - K_{0,-1}(1 + J_{-1,-1})K_{0,-1}]B\rho, \tag{3.6}$$

and we define $K \equiv K_{0,0} - K_{0,-1}(1 + J_{-1,-1})K_{0,-1}$.

We will solve these equations by Fourier methods. Thus let us define the Fourier transform of $f(k)$ as

$$\tilde{f}(\alpha) = \frac{1}{2\pi} \int_{-\infty}^{\infty} e^{-i\alpha k} f(k)dk, \tag{3.7}$$

and the inverse Fourier transform by

$$f(k) = \int_{-\infty}^{\infty} e^{ik\alpha}\tilde{f}(\alpha)d\alpha. \tag{3.8}$$

The convolution is defined as

$$(g * f)(k) = \int_{-\infty}^{\infty} g(k-h)f(h)dh, \tag{3.9}$$

and so $\widetilde{g * f} = 2\pi \tilde{g}\tilde{f}$. The Fourier transformed Equation (3.6) now reads as

$$\tilde{\zeta} = \tilde{\rho} + 2\pi \tilde{K} \tilde{B} \rho, \tag{3.10}$$

where

$$\tilde{K} = \tilde{K}_{0,0} - 2\pi \tilde{K}_{0,-1}^2 / (1 + 2\pi \tilde{K}_{-1,-1}). \tag{3.11}$$

This is an integral operator with kernel

$$K(k) = \int_{-\infty}^{\infty} \tilde{K}(\alpha) e^{ik\alpha} d\alpha, \tag{3.12}$$

and defining $2\pi K(k) \equiv \theta'_{0,0}(k) - \Psi'(k) \equiv \theta'(k)$, we have

$$\Psi'(k) = \int_{-\infty}^{\infty} \frac{[2\pi \tilde{K}_{0,-1}]^2}{1 + 2\pi \tilde{K}_{-1,-1}} e^{ik\alpha} d\alpha. \tag{3.13}$$

Let us write out the kernels, i.e.,

$$K_{0,-1}(k) = \frac{1}{2} \frac{\sin(\pi s)}{\cosh(\pi k) - \cos(\pi s)}, \tag{3.14}$$

$$K_{-1,-1}(k) = -\frac{1}{2} \frac{\sin(2\pi s)}{\cosh(\pi k) - \cos(2\pi s)}. \tag{3.15}$$

However, from [13], we then immediately know the Fourier transforms of these kernels, i.e.,

$$2\pi \tilde{K}_{0,-1}(\alpha) = -\frac{\sinh[\alpha(1+s)]}{\sinh(\alpha)}, \tag{3.16}$$

$$2\pi \tilde{K}_{-1,-1}(\alpha) = \frac{\sinh[\alpha(1+2s)]}{\sinh(\alpha)}. \tag{3.17}$$

Therefore, the kernel $\theta'(k)$ is given as

$$\theta'(k) = \theta'_{00}(k) - 1/2 \int_{-\infty}^{\infty} dt e^{ikt} \frac{\sinh t(1+s)}{\sinh t \cosh ts}. \tag{3.18}$$

We substitute this back into the particle equation, giving a single integral equation for the distribution of particles $\rho(k)$:

$$\frac{1}{2\pi} = \rho(k) + \frac{1}{2\pi} \int_{-B}^{B} \theta'(k-h)\rho(h)dh. \tag{3.19}$$

Then, as usual, energy and momentum are given by

$$P/L = \int_{-B}^{B} \rho(k)k dk = 0, \tag{3.20}$$

$$E/L = \frac{1}{2} \int_{-B}^{B} \rho(k)k^2 dk. \tag{3.21}$$

We have solved the particle equation numerically for ρ. In Figure (3.1), we show E_0/L versus N/L for $s = -1/2$.
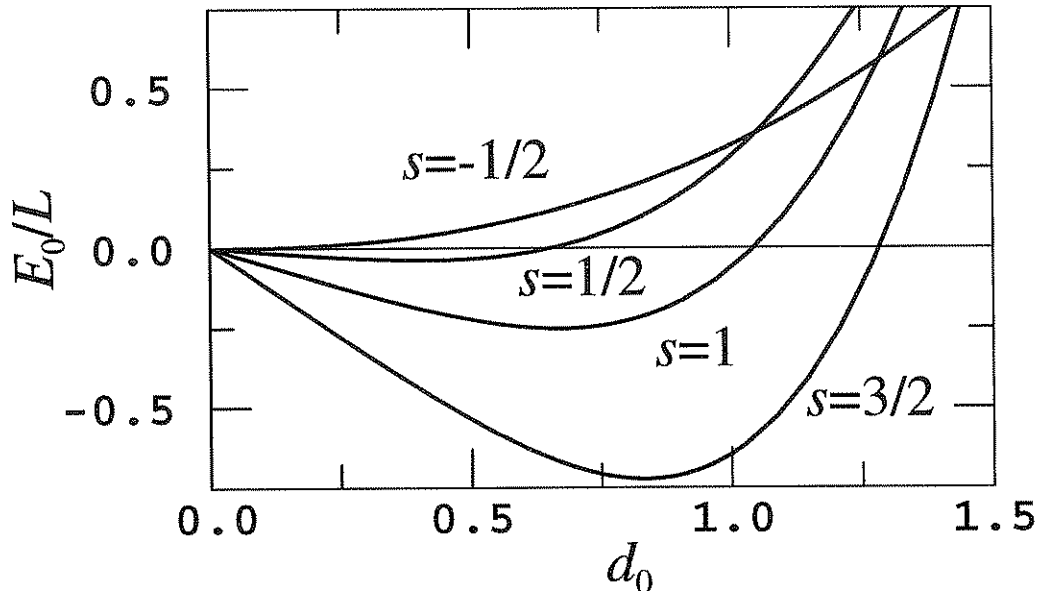
Figure 3.1. Ground state energy per unit length E_0/L versus density N/L for the unbound case at $s = -1/2$ and the bound case at $s = 1/2, 1, 3/2$.

3.1.2   Exited States

Having determined the ground state properties of the system, we now determine the low-energy excited states. They are given by the following: (i) Remove a particle from the ground state distribution, and place it outside the limits; we call this creating a hole and a particle, and it gives a two parameter continuum. (ii) Remove a spin wave from the ground state distribution, and place it on the line with imaginary part equal to i; we call this creating two spin waves, one with spin up and the other with spin down. It gives a two parameter continuum of the type familiar from the Heisenberg-Ising model [13].

By the techniques of Yang and Yang [10], the dispersion relations for particles and holes are given parametrically by

$$\Delta P_0 = q - \int_{-B}^{B} \theta(q-k)\rho(k)dk, \quad \text{for all } q, \tag{3.22}$$

$$= 2\pi \int_{0}^{q} \rho(k)dk, \quad |q| \leq B; \tag{3.23}$$

$$\Delta E_0 = q^2/2 - \frac{1}{2\pi} \int_{-B}^{B} \theta'(q-k)\epsilon(k)dk, \quad \text{for all } q, \tag{3.24}$$

$$= \epsilon(q) + \mu, \quad |q| \leq B. \tag{3.25}$$

Particle-like excitations correspond to $|q| > B$, whereas hole-like excitations correspond to $|q| \leq B$. The spin wave dispersion relations are

$$\Delta P = \int_{-B}^{B} \phi(q-k)\rho(k)dk, \tag{3.26}$$

$$\Delta E = -\frac{1}{2\pi} \int_{-B}^{B} \phi'(q-k)\epsilon(k)dk, \tag{3.27}$$

and hold for all q. Here $\epsilon(k)$ is the solution to the integral equation

$$k^2/2 - \mu = \epsilon(k) + \frac{1}{2\pi} \int_{-B}^{B} \theta'(k-h)\epsilon(h)dh, \tag{3.28}$$

and $\phi'(k) = \frac{\pi}{2s\cosh(\pi k/2s)}$. The results of a numerical solution of these equations are shown in Figure (3.2), for $s = -1/2$, $B = 1$, $d = N/L = 0.600$, $E_0/L = 0.094$, $\mu = 0.374$.

3.1.3 Excitation Velocities

Each of these two types of two-particle continua has an excitation velocity given by the slope of the dispersion relations. The velocity of excitation (i) is then given as

$$v_0(q) = \frac{d(\Delta E)/dq}{d(\Delta P)/dq} = \epsilon'(q)/2\pi\rho(q). \tag{3.29}$$

Let us call $v_0 \equiv v_0(B)$ the *Fermi velocity* of this excitation. In Figure (3.3), we show v_0 as a function of s for various densities.

Figure 3.2. Energy above the ground state energy versus momentum (dispersion relations) for the low lying excitations when $s = -1/2$ and density $N/L = 0.600$.

Figure 3.3. Particle-hole excitation velocity v_0 as a function of particle density d_0 for various interaction strength values s. $s = -0.95$ for the longest dashed curve and increases in increments of 0.13 up to $s = -0.02$. The solid curve corresponds to the noninteracting case, i.e., $v_0(s = 0) = \pi d_0/2$.

The excitation velocity of (ii) is more complicated. Using the spin wave dispersion results and Equation (3.29), we integrate by parts and obtain the Fermi velocity

$$v_{-1} \equiv \frac{1}{2\pi} \frac{\int_{-B}^{B} e^{-\pi k/2s} \epsilon'(k) dk}{\int_{-B}^{B} e^{-\pi k/2s} \rho(k) dk}. \tag{3.30}$$

As has been pointed out in [41], the two velocities are in general not identical. The same is true of the Hubbard model with repulsive on-site interaction, and we will make extensive use of the conformal results obtained for this model [49, 50, 51, 53] in the next chapter. In Figure (3.4), we show v_{-1} as a function of s for various densities.

3.2 The Bound Case

3.2.1 The Ground State

For $s > 0$, which we call the *bound case*, the ground state in the zero sector consists of a spin fluid of type $m = 1$, and thus spin 0. This is the bound state with lowest binding energy, when $\kappa = s$, and so $P(k) = 2k$ and $E(k) = k^2 - s^2$. The finite size Bethe Ansatz equations that describe the ground state may be written as

Figure 3.4. Spin wave-spin wave excitation velocity v_{-1} as a function of particle density d_0 for various interaction strength values s. $s = -0.95$ for the longest dashed curve and increases in increments of 0.13 up to $s = -0.02$. The solid curve corresponds to the noninteracting case, i.e., $v_{-1}(s = 0) = \pi d_0/2 = \pi d_{-1}$.

$$2Lk_j = 2\pi H_j(k_j) + \sum_{l=1}^{N/2} \theta_{1,1}(k_j - k_l). \tag{3.31}$$

Note here that k_j is the pseudo-momentum of a pair, and is not the pseudo-momentum of an individual particle, which would be complex and of the form $k_j/2 \pm is$.

Let us again take the thermodynamic limit. Then in the ground state, the k's for the pairs distribute themselves densely with a density $\tau(k)$, between limits $\pm D$, normalized so that

$$d_1 \equiv N_1/L = \int_{-D}^{D} \tau(k)\mathrm{d}k = N/2L. \tag{3.32}$$

The energy and momentum are given by

$$P/L = 2\int_{-D}^{D} \tau(k)k\mathrm{d}k = 0, \tag{3.33}$$

$$E/L = \int_{-D}^{D} \tau(k)k^2\mathrm{d}k - s^2 N_1/L. \tag{3.34}$$

The integral equation which determines $\tau(k)$ is

$$1/\pi = \tau(k) + \frac{1}{2\pi}\int_{-D}^{D} \theta_{11}'(k - h)\tau(h)\mathrm{d}h. \tag{3.35}$$

The kernel of the equation, $\theta'_{11}(k)$, is the derivative of the phase shift for pair-pair scattering. In Figure (3.1) we show E_0/L versus N/L for selected values of $s = 1/2, 1, 3/2$.

3.2.2 Excited States

The low-energy excited states are given by the following: (i) Remove a pair from the ground state distribution, and place it outside the limits; we call this creating a pair-hole and a pair, and it gives a two parameter continuum. (ii) Break a pair, to give two particles, one spin up and the other spin down; this also gives a two parameter continuum. (iii) Excite a pair into a higher energy bound state, if allowed; these we call *excitons*, and they have single parameter dispersion relations. The dispersion relations are given parametrically by

$$\Delta P = \sum_m \left[\eta_m k_m - \int_{-D}^{D} \theta_{m1}(k_m - k)\rho(k)\mathrm{d}k \right], \tag{3.36}$$

$$\Delta E = \sum_m \left[\frac{\eta_m k_m^2}{2} - \frac{1}{2\pi} \int_{-D}^{D} \theta'_{m1}(k_m - k)\epsilon(k)\mathrm{d}k \right]. \tag{3.37}$$

Here $\epsilon(k)$ is the solution to the integral equation

$$k^2 - s^2 = \mu_1 = \epsilon(k) + \frac{1}{2\pi} \int_{-B}^{B} \theta'_{11}(k - k')\epsilon(k')\mathrm{d}k'. \tag{3.38}$$

The chemical potential μ_1 is the chemical potential for pairs, given by $\partial E_0/\partial N_1$.

Again, we have solved these integral equations numerically. The results are shown in Figure (3.5) for $s = 3/2$, $B = 3/2$, $d = N/L = 0.943$, $E_0/L = -0.691$, $\mu_1 = 1.215$. The gap for the creation of two particles is $\Delta E = 1.170$, and is equal to the discontinuity of the chemical potential across the line $N_\uparrow = N_\downarrow$. The exciton with $m = 2$ is the only exciton allowed at this value of s, and has a gap of $\Delta E = 1.017$.

3.2.3 Excitation Velocity

Let us denote the Fermi velocity of the excitations of type (i) by

$$v_1 \equiv \epsilon'(D)/2\pi\tau(D). \tag{3.39}$$

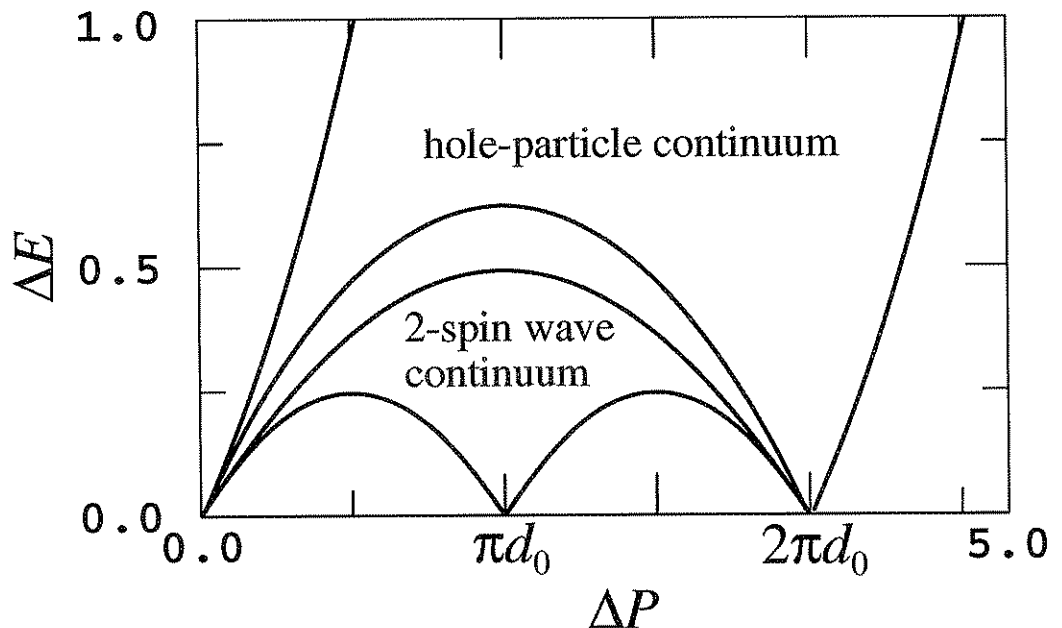In Figure (3.6), we show v_1 as a function of s for various densities.
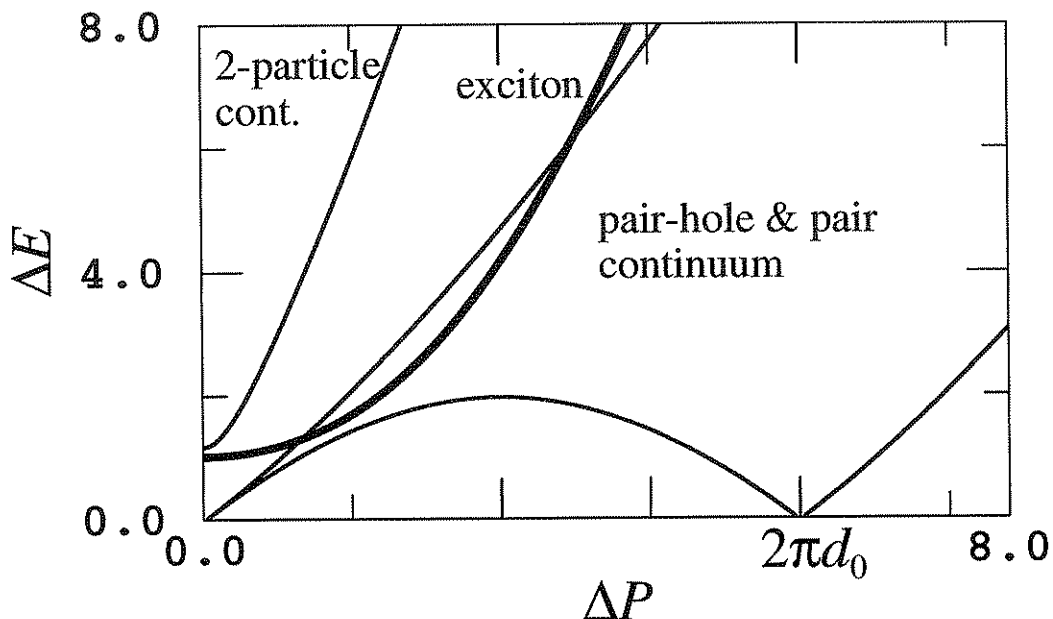
Figure 3.5. Energy above the ground state energy versus momentum (dispersion relations) for the low lying excitations when $s = 3/2$ and density $N/L = 0.943$.
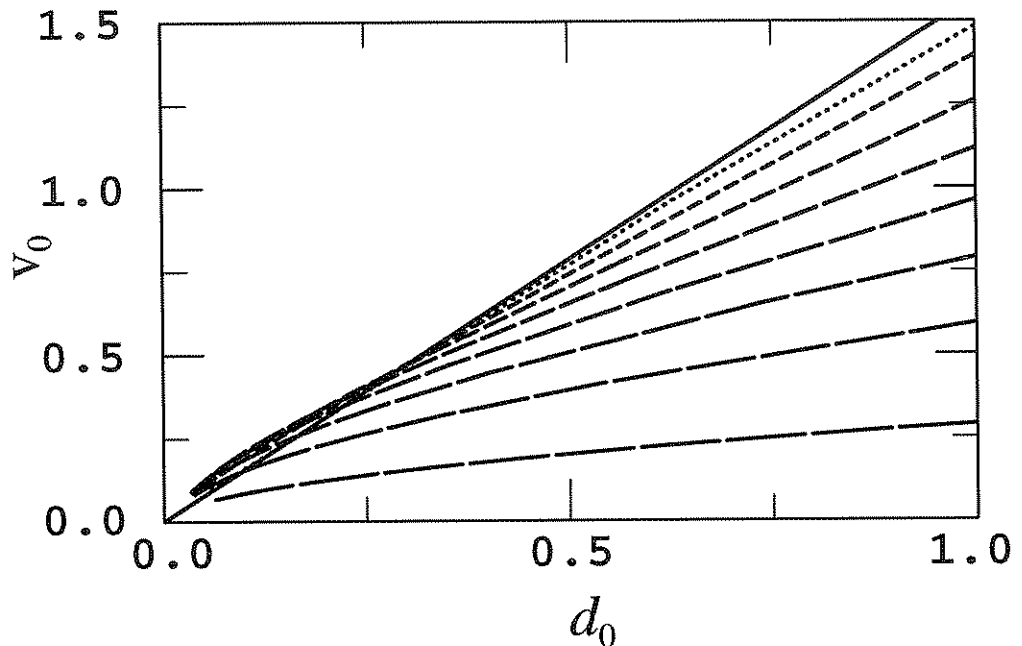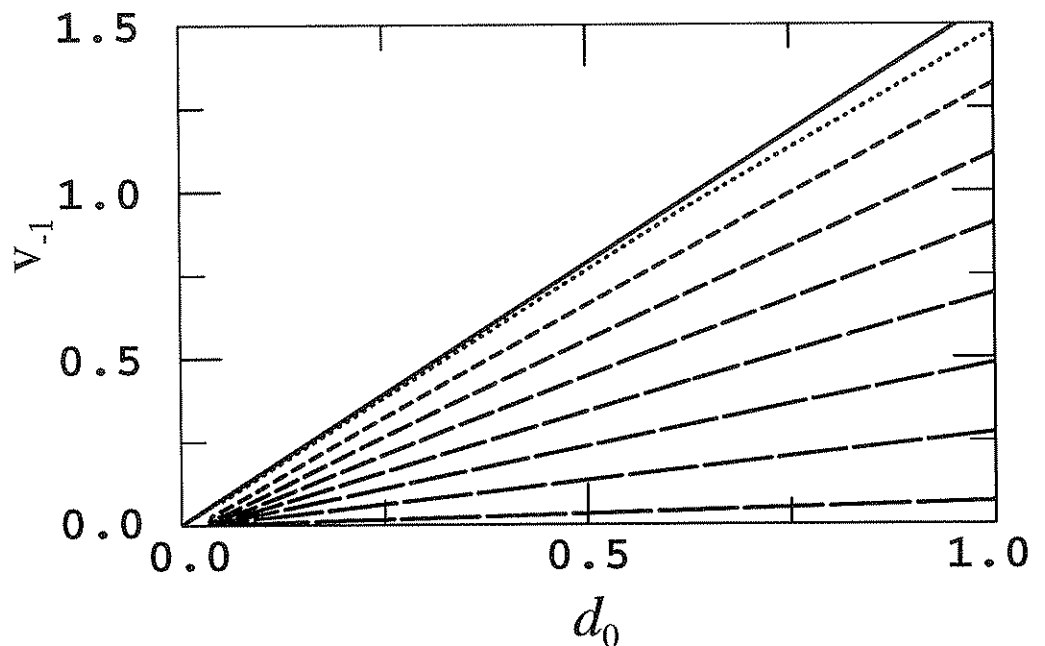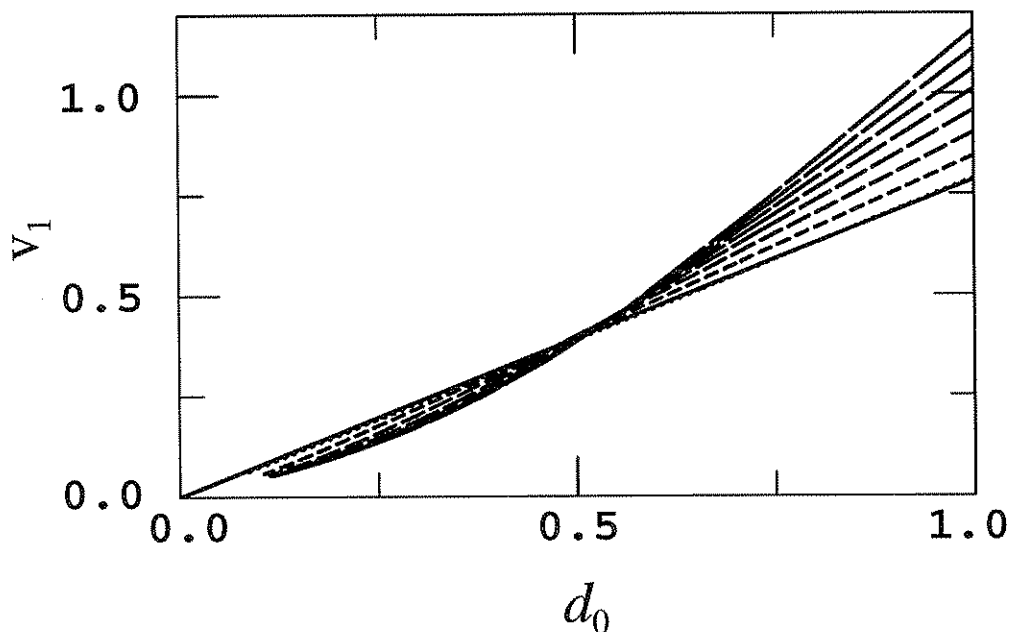

Figure 3.6. Pair-pair hole excitation velocity v_1 as a function of particle density d_0 for various interaction strength values s. $s = 0.95$ for the longest dashed curve and decreases in increments of -0.13 up to $s = 0.02$. The solid curve corresponds to the noninteracting case, i.e., $v_1(s = 0) = \pi d_1/2$.

CHAPTER 4

CORRELATION FUNCTIONS FOR THE ZERO SECTOR

The concept of conformal invariance in one-dimensional quantum systems at criticality constrains the possible asymptotic behavior of correlation functions and allows a classification into universality classes, distinguished by the value of the central charge c of the underlying Virasoro algebra [42, 43, 44]. For models with short-range interactions and a gapless excitation spectrum with a single excitation velocity, we can determine both c and the critical exponents of correlators directly from finite-size corrections to the ground state energy and the low-lying exited states. In most cases, such models have been found to belong to the universality class of the one-dimensional Tomonaga-Lieb-Mattis-Luttinger model [45, 46, 47, 48], i.e., $c = 1$, and the critical exponents to vary as functions of the coupling constant of the corresponding conformal theory.

Recently, various authors have extended these concepts to include multicomponent systems with different excitation velocities, such as the Hubbard model [49, 50, 51, 52, 53]. In general, one finds a $c = 1$ Virasoro algebra for each critical degree of freedom, i.e., each gapless excitation with a unique velocity. It is then possible to construct the full theory as a semidirect product of these independent algebras. Again, critical exponents may be calculated from finite-size corrections but now they are functions of a matrix of coupling constants.

In another recent development, the ideas of conformal field theory have been applied to models with long-range interactions such as the $1/r^2$ system [54, 55, 56]. It turns out that one can no longer simply read off the value of the central charge from the finite-size corrections to the ground state energy. However, one may still calculate the correct critical exponents of the asymptotics of the correlations functions from the finite-size scaling behavior of the low-lying excitations [57].

4.1 Conformal Approach for Correlation Functions

Let us recall the basic ideas for calculating the correlation functions and their critical exponents [66]. Every primary field $\phi_\pm$ in a conformal field theory on an infinite strip of width L in the space direction gives rise to a tower of exited states. Let $x = \Delta^+ + \Delta^-$ denote the scaling dimension and $\sigma = \Delta^+ - \Delta^-$ the spin of $\phi_\pm$. Then the energies and momenta of these exited states scale as

$$E(\Delta^\pm, N^\pm) - E_0 \quad \sim \quad \frac{2\pi v}{L}(x + N^+ + N^-), \tag{4.1}$$

$$P(\Delta^\pm, N^\pm) - P_0 \quad \sim \quad \frac{2\pi}{L}(\sigma + N^+ - N^-) + 2Dk_f. \tag{4.2}$$

Here E_0 is the ground state energy of the finite system, N^+ and N^- are positive integers, v is the common Fermi velocity of the excitations and $2D$ is the momentum of the state in units of the Fermi momentum k_f. The so-called conformal weights $\Delta^\pm$ will in general be dependent on the number of particles N as well as D and $N^\pm$. Furthermore, the explicit functional behavior $\Delta^\pm(N, D, N^\pm)$ is governed by the value of the central charge c. For $c = 1$, the interaction strength of the model under consideration changes the weights $\Delta^\pm$, too.

We may then write the correlation functions of the primary fields at zero temperature (expressions for low but finite temperature may also be given) as

$$\langle \phi_{\Delta^\pm}(x,t)\phi_{\Delta^\pm}(0,0) \rangle = \frac{\exp(-2iDk_f x)}{(x - ivt)^{2\Delta^+}(x + ivt)^{2\Delta^-}}. \tag{4.3}$$

We remark that for a box of finite length L the correlator has to be periodic in L and the above formula should be replaced by

$$\langle \phi_{\Delta^\pm}(x,t)\phi_{\Delta^\pm}(0,0) \rangle = \frac{\exp(-2iDk_f x)}{\sinh[\pi(vt - ix)/L]^{2\Delta^+} \sinh[\pi(vt - ix)/L]^{2\Delta^-}}. \tag{4.4}$$

As has been shown in [57], this form is important for comparison with numerical studies of particles confined to a finite ring.

Now, let $\mathcal{O}_{\Delta N}(x,t)$ be a local operator which changes the number of particles by ΔN. Then from [50], we know that the asymptotics of the correlator $\langle \mathcal{O}_{-\Delta N}(x,t)\mathcal{O}_{\Delta N}(0,0) \rangle$ may be written as an expansion in correlators of primary fields $\phi_\pm$ such that

$$\langle \mathcal{O}_{-\Delta N}(x,t)\mathcal{O}_{\Delta N}(0,0) \rangle \sim \sum_{D,N^\pm} \prod_\pm \langle \phi_{\Delta^\pm}(x,t)\phi_{\Delta^\pm}(0,0) \rangle, \tag{4.5}$$

for ΔN fixed. The leading asymptotic behavior is then given by minimizing the critical exponents w.r.t. D and nonzero D will lead to oscillatory behavior.

However, the excitation spectrum of the SC model is quite different for the bound $(s > 0)$ and the unbound $(-1 < s < 0)$ case as we have argued in the previous section. Most importantly, the unbound case does not have a common velocity for all excitations anymore, and so the formulas given above for a Lorentz-invariant conformal field theory can no longer hold.

4.2   The Central Charge

Following the arguments of the last section, we should first establish the value of the central charge for the SC model. This is usually done with the help of the finite-size scaling formula,

$$E_0 \sim \epsilon_0 L - \frac{\pi v}{6L} c. \tag{4.6}$$

Here, ϵ_0 is the ground state energy density in the thermodynamic limit. In short-ranged one-dimensional quantum models, including Bethe-Ansatz solvable models, $c = 1$ as mentioned above [61, 62]. However, for long-ranged models, straightforward application of this equation leads to unphysical results [56]. (We include the SC model in this class, although its pair potential decays exponentially, since it can only be solved by means of the *asymptotic* Bethe Ansatz.) For instance, in the $1/r^2$ models c is predicted to be equal to the interaction strength, although independent calculations show that the critical exponents are those of the $c = 1$ universality class [57]. However, if one instead estimates c from the low temperature expansion of the free energy [58, 59], one does get the correct answer $c = 1$ and

$$F(T) \simeq F(T = 0) - \frac{\pi T^2}{6v}. \tag{4.7}$$

Let us look at the central charge of the SC model for the unbound case. As pointed out in the last chapter, there are two gapless excitations with different velocities each. Thus following the arguments of [60], we expect one $c = 1$ Virasoro algebra for each excitation and thus Equation (4.6) is generalized to

$$E_0 \sim \epsilon_0 L - \left(\frac{\pi v_0}{6L} - \frac{\pi v_{-1}}{6L} \right) c. \tag{4.8}$$

We have iterated the Bethe Ansatz Equations (3.1) for finite systems in the ground state and calculated the energy $E_0(L)$. Using ϵ_0 and the velocities v_0, v_{-1} as calculated in the preceding chapter from the integral equations, we may estimate c for different interaction strength s from a finite-size plot. In Figure (4.1), we show the results for lattice sizes $L = 4, 8, 12, \ldots, 32$. (The reader should compare this result with the finite-size analysis
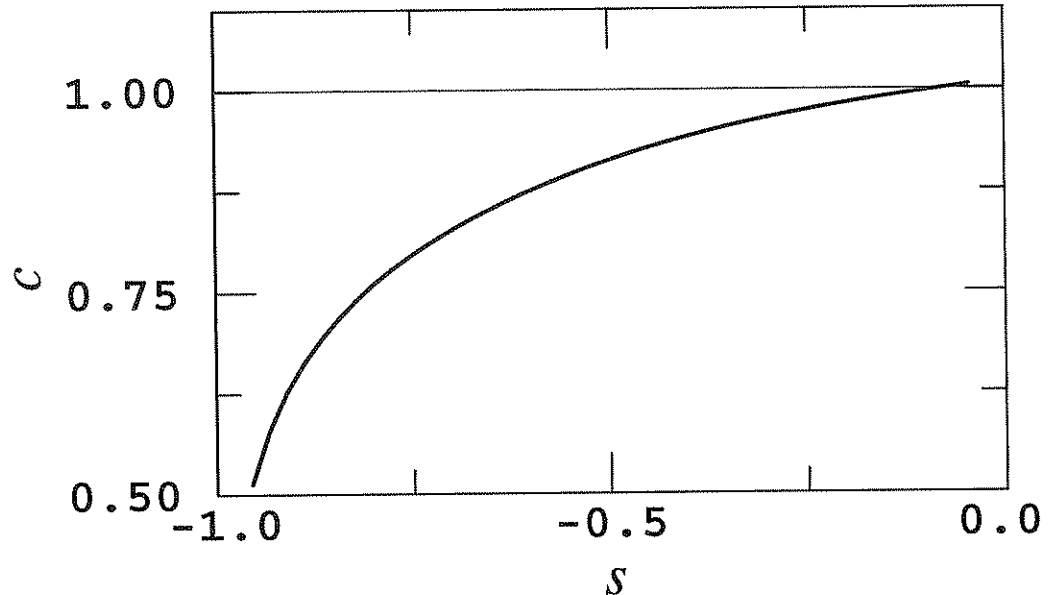
Figure 4.1. The central charge of the SC model as a function of the interaction strength s. Note that $c \simeq 1$ only for the noninteracting case $s = 1$.

of Chapter 5 and especially Figure (5.6)). As for the periodic $1/r^2$ model, the standard finite-size formula gives $c = 1$ only for the noninteracting case $s = 0$.

Let us discuss some possible explanations for this contradiction. We have previously argued [57] that long-ranged models "feel" the finite-size constraint much more strongly than short-ranged systems and thus an additional boundary energy term should appear in Equation (4.6). Boundary conditions for Equation (4.7) effect the time axis only, thus explaining its success. However, all of the long-ranged models of the $1/r^2$ type show a perfectly reasonable thermodynamic limit and it seems improbable that boundary effects play such a paramount role. Indeed, being able to take the thermodynamic limit $L \to \infty$ at fixed density is at the heart of the asymptotic Bethe Ansatz.

One might now argue that, since the asymptotic Bethe Ansatz is only supposed to be exact in the thermodynamic limit, the deviations are due to Equation (4.6) not being correct for the asymptotic Bethe Ansatz. This, however, cannot be true for the periodic $1/r^2$ model, where the ground state energy is known exactly [20].

Now, let us make the case for $c = 1$ on more general grounds. The behavior of the correlation for a given one-dimensional model at large distances and low-temperatures is determined by the gapless excitations [63]. These gapless excitations are due to

hydrodynamic density fluctuations and their quasi-particle structure is mostly either given by phonons or particles and holes.

The dispersion relation close to the pseudo-Fermi momentum is generically linear, i.e., $\epsilon(k) = v|k|$ with $k = 2\pi n/L$ and n an integer. The phonons obey Bose statistics such that their momentum distribution — and not the pseudo-momentum distribution ρ of Chapter 3 — is $n_B(k) = 1/(e^{\epsilon/T} - 1)$. But then we easily calculate

$$
\begin{aligned}
\Delta E &= \frac{L}{2\pi} \int_{-\infty}^{\infty} \epsilon(k) n_B(k) dk \\
&= \frac{vL}{\pi} \int_{-\infty}^{\infty} \frac{k}{e^{vk/T} - 1} dk \\
&= \frac{T^2 L}{\pi v} \int_{-\infty}^{\infty} \frac{x}{e^x - 1} dx \\
&= \frac{\pi T^2 L}{6v},
\end{aligned}
\tag{4.9}
$$

and comparison with Equation (4.6) gives $c = 1$.

Suppose now that we have a particle-hole continuum and the two types of quasi-particles obey Fermi statistics. For both particles and holes, v will be the same and again, we can calculate the low-temperature correction to the thermodynamics. This time, however, we have two types of fermions, so

$$
\begin{aligned}
\Delta E &= \frac{L}{\pi} \int_{-\infty}^{\infty} \epsilon(k) n_F(k) dk \\
&= \frac{2vL}{\pi} \int_{-\infty}^{\infty} \frac{k}{e^{vk/T} + 1} dk \\
&= \frac{2T^2 L}{\pi v} \int_{-\infty}^{\infty} \frac{x}{e^x + 1} dx \\
&= \frac{\pi T^2 L}{6v}.
\end{aligned}
\tag{4.10}
$$

Again we have $c = 1$. Interactions between particles and holes can be neglected, since the number of particles (holes) will be rather small for low temperatures, i.e.,

$$
\begin{aligned}
\delta N &= \frac{L}{2\pi} \int_{-\infty}^{\infty} n_F(k) dk \\
&= \frac{L}{\pi} \int_{-\infty}^{\infty} \frac{k}{e^{vk/T} + 1} dk \\
&= \frac{TL}{\pi v} \int_{-\infty}^{\infty} \frac{x}{e^x + 1} dx \\
&= \frac{TL \log 2}{\pi v}.
\end{aligned}
\tag{4.11}
$$

Assuming our above arguments are correct and we may indeed read off the critical anomaly $c = 1$ from the finite-temperature corrections, we still have to explain what

could be wrong with Equation (4.6). Let us thus put forward a few suggestions: To the best of the authors knowledge, there is actually no direct derivation of Equation (4.6) by conformal field theory, in contrast to Equation (4.7) [58, 59]. Equation (4.6) is then derived from Equation (4.7) by noting that the free energy of a classical two-dimensional system may be viewed as the ground state energy ϵ_0 of a corresponding, although in general not identical, one-dimensional quantum system [64, 65]. However, the derivation of this correspondence is done for the case of a lattice model with *isotropic* interaction in both space and time directions. The classical two-dimensional models corresponding to the $1/r^2$ model and the SC model are not known, but due to the long-ranged character of the interactions, there will be an anisotropy of space and time directions. Indeed it has been shown that for even short-ranged lattice models with anisotropy, Equation (4.6) is no longer true and the value of c has to be rescaled by the anisotropy strength [66]. Furthermore, the $1/r^2$ model and the SC model are both *continuum* models and it is thus not clear whether the results of [64, 65] should be expected to hold at all.

Let us conclude this section by reemphasizing that although we believe $c = 1$ to be the correct value of the critical anomaly by the above given general arguments and we use it in the following [67], there is no satisfactory proof and further study is needed.

4.3 Asymptotic Correlation Functions for the Unbound Case

4.3.1 The Dressed Charge Matrix

For the unbound case, two excitation branches are gapless, giving rise to a particle-hole continuum and to a spin wave continuum, with Fermi velocities v_0 and v_{-1}, respectively. Thus, the finite size corrections of Equations (4.1) and (4.2) need to be generalized. Their new form now are [50, 53],

$$
\begin{aligned}
E(\Delta \mathbf{N}, \mathbf{D}) - E_0 \sim & \\
& \frac{2\pi}{L} \left[\frac{1}{4} \Delta \mathbf{N}^T (\Xi^{-1})^T V (\Xi^{-1}) \Delta \mathbf{N} + \mathbf{D}^T \Xi V \Xi^T \mathbf{D} \right] \\
& + \frac{2\pi}{L} \left[v_0 (N_0^+ + N_0^-) + v_{-1} (N_{-1}^+ + N_{-1}^-) \right],
\end{aligned} \tag{4.12}
$$

$$
\begin{aligned}
P(\Delta \mathbf{N}, \mathbf{D}) - P_0 \sim & \\
& \frac{2\pi}{L} \left[\Delta \mathbf{N}^T \, \mathbf{D} + N_0^+ - N_0^- + N_{-1}^+ - N_{-1}^- \right] \\
& + 2 D_0 k_{f,\uparrow} + 2(D_0 + D_{-1}) k_{f,\downarrow}.
\end{aligned} \tag{4.13}
$$

Here, the matrix $V \equiv \mathrm{diag}(v_0, v_{-1})$ and the excited state is characterized by the pairs $\Delta N = (\Delta N_0, \Delta N_{-1})$ and $\mathbf{D} = (D_0, D_{-1})$. As before, $N_0^{\pm}$ and $N_{-1}^{\pm}$ are positive integers that label the descendant fields. The 2×2 matrix Ξ is called the *dressed charge matrix* [50, 53] and may be calculated by means of coupled integral equations. Thus if we denote the components of Ξ by

$$\Xi = \begin{pmatrix} \xi_{0,0}(B) & \xi_{0,-1}(C) \\ \xi_{-1,0}(B) & \xi_{-1,-1}(C) \end{pmatrix}, \tag{4.14}$$

then

$$\xi_{0,0}(k) =$$
$$1 - \frac{1}{2\pi} \int_{-B}^{B} \xi_{0,0}(h) \theta'_{0,0}(h - k) dh - \frac{1}{2\pi} \int_{-C}^{C} \xi_{0,-1}(\mu) \theta'_{-1,0}(\mu - k) d\mu, \tag{4.15a}$$

$$\xi_{0,-1}(\lambda) =$$
$$0 - \frac{1}{2\pi} \int_{-B}^{B} \xi_{0,0}(h) \theta'_{0,-1}(h - \lambda) dh - \frac{1}{2\pi} \int_{-C}^{C} \xi_{0,-1}(\mu) \theta'_{-1,-1}(\mu - \lambda) d\mu, \tag{4.15b}$$

$$\xi_{-1,0}(k) =$$
$$0 - \frac{1}{2\pi} \int_{-B}^{B} \xi_{-1,0}(h) \theta'_{0,0}(h - k) dh - \frac{1}{2\pi} \int_{-C}^{C} \xi_{-1,-1}(\mu) \theta'_{-1,0}(\mu - k) d\mu, \tag{4.15c}$$

$$\xi_{-1,-1}(\lambda) =$$
$$1 - \frac{1}{2\pi} \int_{-B}^{B} \xi_{-1,0}(h) \theta'_{0,-1}(h - \lambda) dh - \frac{1}{2\pi} \int_{-C}^{C} \xi_{-1,-1}(\mu) \theta'_{-1,-1}(\mu - \lambda) d\mu. \tag{4.15d}$$

Thus, the situation for $-1 < s < 0$ is analogous to the situation in the repulsive Hubbard model away from half-filling [53, 49] and we may interpret Equations (4.13) and (4.13) in terms of a semidirect product of two independent Virasoro algebras, both with $c = 1$. The formulas for the conformal weights $\Delta_0^{\pm}$ and $\Delta_{-1}^{\pm}$ as functions of the components of the dressed charge matrix Ξ are given as

$$\Delta_0^{\pm}(\Delta N, \mathbf{D}) = \frac{1}{2} \left[\xi_{0,0} D_0 + \xi_{-1,0} D_{-1} \pm \frac{\xi_{-1,-1} \Delta N_0 - \xi_{0,-1} \Delta N_{-1}}{2 \det \Xi} \right]^2,$$

$$\Delta_{-1}^{\pm}(\Delta N, \mathbf{D}) = \frac{1}{2} \left[\xi_{0,-1} D_0 + \xi_{-1,-1} D_{-1} \pm \frac{\xi_{0,0} \Delta N_{-1} - \xi_{-1,0} \Delta N_0}{2 \det \Xi} \right]^2. \tag{4.16}$$

The generalization of the correlation functions of the primary fields as in Equation (4.3) is

$$\frac{\exp(-2i D_0 k_{f,\uparrow} x) \exp[-2i(D_0 + D_{-1}) k_{f,\downarrow} x]}{(x - i v_0 t)^{2\Delta_0^+} (x + i v_0 t)^{2\Delta_0^-} (x - i v_{-1} t)^{2\Delta_{-1}^+} (x + i v_{-1} t)^{2\Delta_{-1}^-}}. \tag{4.17}$$

For the zero sector, i.e., $\mathcal{M} = 0$, the relevant equations simplify considerably. In this case, $k_{f,\downarrow} = k_{f,\uparrow} \equiv k_f = \pi d_0/2$, and the dressed charge matrix Ξ may again be expressed in terms of a single parameter $\xi_0 \equiv \xi_0(B)$, i.e.,

$$\Xi = \begin{pmatrix} \xi_0 & 0 \\ \frac{1}{2}\xi_0 & \frac{1}{\sqrt{2(1+s)}} \end{pmatrix}. \tag{4.18}$$

Let us demonstrate how to arrive at this result. We will again use the operator notation developed in the last chapter. Equation (4.15) in the zero sector is

$$\zeta = \xi_{0,0} + K_{0,0}B\xi_{0,0} + K_{0,-1}\xi_{0,-1}, \tag{4.19a}$$

$$0 = \xi_{0,-1} + K_{0,-1}B\xi_{0,0} + K_{-1,-1}\xi_{0,-1}, \tag{4.19b}$$

$$0 = \xi_{-1,0} + K_{-1,0}B\xi_{-1,0} + K_{-1,0}\xi_{-1,-1}, \tag{4.19c}$$

$$\zeta = \xi_{-1,-1} + K_{-1,-1}B\xi_{-1,0} + K_{-1,-1}\xi_{-1,-1}. \tag{4.19d}$$

Let us consider Equations (4.19a) and (4.19b). We rewrite Equation (4.19b) with the help of the resolvent such that $\xi_{0,-1} = -(1 + J_{-1,-1})K_{0,-1}B\xi_{0,0}$ and put it back into Equation (4.19a), so that

$$[1 + (K_{0,0} + K_{-1,0}(1 + J_{-1,-1})K_{0,-1})B]\,\xi_{0,0} = \zeta \tag{4.20}$$

Keeping in mind that $K_{mm'} = K_{m'm}$, this is identical to Equation (3.6) and thus we immediately have an integral equation for $\xi_0(k) \equiv \xi_{0,0}(k)$,

$$\xi_0(k) = 1 - \frac{1}{2\pi}\int_{-B}^{B}\xi_0(h)\theta'(h - k)dh, \tag{4.21}$$

where the kernel is as in Equation (3.18).

Turning now to the second pair of equations, we again use the resolvent to solve for $\xi_{-1,-1}$ and plug it back into Equation (4.19c). This then gives us the equation

$$[1 + (K_{0,0} + K_{-1,0}(1 + J_{-1,-1})K_{0,-1})B]\,\xi_{-1,0} = -K_{-1,0}(1 + J_{-1,-1})\zeta \equiv \zeta'. \tag{4.22}$$

This is very close to Equation (4.20), the only difference being the constant on the right hand side. However, the right hand side can be calculated explictly and the result is $\zeta' = 1/2$. Therefore, we immediately have the desired relation $\xi_{-1,0}(k) = \xi_{0,0}(k)/2$.

We are thus left with evaluating the last column. The $\xi_{0,-1}(k)$ entry can easily be shown to be 0 for all k. Let us then turn to $\xi_{-1,-1}$. The integral equation to be solved is

$$\xi_{-1,-1}(k) + \frac{1}{2\pi}\int_{-B}^{B}\xi_{-1,-1}(h)\theta'_{-1,-1}(h - k)dh = 1. \tag{4.23}$$

We may avoid a long Wiener-Hopf type calculation, by noting that this equation has been studied previously by Yang and Yang [13]. Following [13] we parameterize the anisotropy

in the Heisenberg-Ising model by $\Delta = -\cos(\mu)$. Then the correspondence is established by setting $\mu = -\pi s$ and we immediately have the result $\xi_{-1,-1}(B) = \sqrt{\pi/2(\pi - \mu)} = 1/\sqrt{2(1 + s)}$ for the SC model in the zero sector.

Then from Equation (4.16), the conformal weights $\Delta_0^{\pm}$ and $\Delta_{-1}^{\pm}$ are given as

$$
\begin{aligned}
\Delta_0^{\pm} &= \frac{1}{2}\xi_0^2 (D_0 + \frac{1}{2}D_{-1})^2 + \frac{1}{8\xi_0^2}(\Delta N_0)^2 \\
&\quad \pm \frac{1}{4}\Delta N_0(2D_0 + D_{-1}) + N_0^{\pm},
\end{aligned}
\tag{4.24}
$$

$$
\begin{aligned}
\Delta_{-1}^{\pm} &= \frac{1}{4(1+s)}(D_{-1})^2 + \frac{(1+s)}{4}(\Delta N_{-1} - \frac{1}{2}\Delta N_0)^2 \\
&\quad \pm \frac{1}{4}(2\Delta N_{-1} - \Delta N_0)D_{-1} + N_{-1}^{\pm}.
\end{aligned}
\tag{4.25}
$$

Note that the second equation is independent of ξ_0. However, there is now an explicit dependence on the interaction strength s and only for $s = 0$ do we recover the result of the Hubbard model.

This s dependence can be understood by realizing that for the zero sector and $-1 < s < 0$ the Bethe-Ansatz equations of the rapidities $\mathbf{k}_{-1} = (\lambda_1, \ldots, \lambda_{N_{-1}})$ are essentially the Bethe-Ansatz equations of the Heisenberg-Ising model. The effect of the Bethe-Ansatz equations for the pseudo-momenta is simply a renormalization. Thus we may say that the behavior of the spin wave excitations changes from ferromagnetic at $s \to -1^+$ ($\Delta = 1$) to antiferromagnetic at $s \to 0^-$ ($\Delta = -1$). Furthermore, we expect to see free spin waves at $s = -1/2$. This picture has been confirmed by a study of the transport properties of the SC model which we present in the next chapter.

Alternatively, we may simply express ξ_0 in terms of thermodynamical response functions. Let us change a given ground state configuration by adding particles while keeping the Fermi sea at zero momentum, so that the excitation can be described by $\Delta N_0 = 2\Delta N_{-1}$ and $\mathbf{D} = (0, 0)$. Then a second order expansion gives

$$
\Delta E = -\mu_0(\Delta N_0) + \frac{1}{2}\frac{1}{L\kappa_0 d_0^2}(\Delta N_0)^2,
\tag{4.26}
$$

where $\mu_0 = -\frac{\partial E}{\partial N_0}$ is the chemical potential for adding particles and κ_0 is the particle-compressibility. Comparison with (4.1) and (4.44) yields

$$
\xi_0^2 = \pi v_0 \kappa_0 d_0^2 = \pi d_0 / v_0.
\tag{4.27}
$$

In the last equation, we have used the well known relation $v_0^2 = 1/(\kappa_0 d_0)$. Therefore, we may calculate the critical exponents of the correlation functions of the SC model in the zero sector by simply using the Fermi velocity v_0 calculated in the last chapter.

4.3.2   Correlators

For $-1 < s < 0$, we want to consider the following set of correlators: Let $\psi_\sigma(x,t)$ denote the field operator of a particle with spin σ. Later, we will additionally restrict the statistics to be either bosonic or fermionic by restricting the possible values of the pair **D**. Then the field correlator — also called the one-particle reduced density matrix — is given by

$$C_\psi(x,t) = \langle \psi_\downarrow(x,t)\psi_\downarrow^\dagger(0,0)\rangle. \tag{4.28}$$

Defining the number operator $n(x,t) = n_\uparrow(x,t) + n_\downarrow(x,t)$, we write the density-density correlator

$$C_n(x,t) = \langle n(x,t)n(0,0)\rangle. \tag{4.29}$$

The spin-spin correlation functions are

$$C_\sigma^z(x,t) = \langle S^z(x,t)S^z(0,0)\rangle, \tag{4.30}$$

$$C_\sigma^\perp(x,t) = \langle S^-(x,t)S^+(0,0)\rangle, \tag{4.31}$$

where we used $S^z = (n_\uparrow - n_\downarrow)/2$ and $S^+ = \psi_\uparrow^\dagger\psi_\downarrow$. Note that for systems that are rotationally invariant, such as the Hubbard model in zero magnetic field, these two spin-spin correlators are closely related, i.e., $C_\sigma^z = 2C_\sigma^\perp$.

Following [53], we also consider the correlation function for singlet pairs,

$$C_{sing}(x,t) = \langle \psi_\uparrow^\dagger(x,t)\psi_\downarrow^\dagger(x,t)\psi_\uparrow(0,0)\psi_\downarrow(0,0)\rangle. \tag{4.32}$$

Note that all these correlators are of the form $\langle A(x,t)A^\dagger(0,0)\rangle$. By standard arguments of conformal field theory [42, 43, 44], we may deduce the leading terms and the critical exponents of the long-distance behavior of these correlators by expanding A in terms of the primary fields $\phi_\pm$ while minimizing with respect to **D** at the corresponding values of Δ**N**. This approach, however, will leave the expansion coefficients undetermined and at special points in the phase diagram, they may even vanish.

The particle quantum numbers I_j and the spin-wave quantum numbers J_α are restricted by the parities of N_0, N_{-1} and the statistics of the particles to the following combination of integers and half-odd integers: If both spin-up and spin-down particles are bosons

$$I_j = (N_0 - 1)/2 \pmod 1,$$

$$J_\alpha = (N_{-1} - 1)/2 \ (\text{mod } 1), \tag{4.33}$$

whereas for fermions,

$$I_j = N_{-1}/2 \ (\text{mod } 1),$$
$$J_\alpha = (N_0 + N_{-1} - 1)/2 \ (\text{mod } 1). \tag{4.34}$$

Due to the restrictions (4.33) and (4.34) on the quantum numbers of a given state, the numbers $\mathbf{D} = (D_0, D_{-1})$ are integers or half-odd integers depending on the parities of the pair $\Delta \mathbf{N} = (\Delta N_0, \Delta N_{-1})$ and the statistics of $\psi^\dagger, \psi$. In particular, for fermionic particles we have

$$D_0 = \frac{\Delta N_0 + \Delta N_{-1}}{2} \ (\text{mod } 1), \quad D_{-1} = \frac{\Delta N_0}{2} \ (\text{mod } 1). \tag{4.35}$$

We can now apply the above scheme for calculating the leading asymptotic behavior of the correlation function. Following our selection rules, we therefore have for a fermionic system

$$
\begin{array}{llll}
C_\psi: & \Delta N_0 = 1; & \Delta N_{-1} = 1; \\
& D_0 = 0, \pm 1, \ldots; & D_{-1} = \pm \frac{1}{2}, \ldots; \\
C_n: & \Delta N_0 = 0; & \Delta N_{-1} = 0; \\
& D_0 = 0, \pm 1, \ldots; & D_{-1} = 0, \pm 1, \ldots; \\
C_\sigma^z: & \Delta N_0 = 0; & \Delta N_{-1} = 0; \\
& D_0 = 0, \pm 1, \ldots; & D_{-1} = 0, \pm 1, \ldots; \\
C_\sigma^\perp: & \Delta N_0 = 0; & \Delta N_{-1} = 1; \\
& D_0 = \pm \frac{1}{2}, \ldots; & D_{-1} = 0, \pm 1, \ldots; \\
C_{sing}: & \Delta N_0 = 2; & \Delta N_{-1} = 1; \\
& D_0 = \pm \frac{1}{2}, \ldots; & D_{-1} = 0, \pm 1, \ldots .
\end{array}
\tag{4.36}
$$

This is identical to the results for the repulsive Hubbard model, and as in [53], we will write the critical exponents as functions of $\theta_0 \equiv 2\xi_0^2$. However, there is an additional interaction strength dependence in the correlation functions due to the explicit appearance of s in Equation (4.25). This is a novel feature and not true in the Hubbard model. It emphasizes the close correspondence of the Heisenberg-Ising model and the SC model for $-1 < s < 0$ in the zero sector.

We now calculate the leading asymptotics of the fermionic field correlator in the SC model to be

$$
\begin{aligned}
C_\psi(x, t) \quad \sim \quad & \frac{1}{|x + iv_0 t|^{1/\theta_0 + \theta_0/16}|x + iv_{-1} t|^{\frac{1}{2} + s^2/4(s+1)}} \\
& \times \text{Re} \left[A_0 e^{-ik_f x} \left(\frac{x + iv_0 t}{x - iv_0 t} \right)^{\frac{1}{4}} \left(\frac{x + iv_{-1} t}{x - iv_{-1} t} \right)^{\frac{1}{4}} \right]
\end{aligned}
$$

$$+ \frac{1}{|x + iv_0 t|^{1/\theta_0 + 9\theta_0/16}|x + iv_{-1}t|^{\frac{1}{2} + s^2/4(s+1)}}$$
$$\times \mathrm{Re}\left[A_1 e^{-i3k_f x}\left(\frac{x + iv_0 t}{x - iv_0 t}\right)^{\frac{3}{4}}\left(\frac{x + iv_{-1}t}{x - iv_{-1}t}\right)^{\frac{1}{4}}\right]. \quad (4.37)$$

The density-density correlator is given by

$$C_n(x, t) \quad \sim \quad n_0^2 + A_1 \frac{\cos(2k_f x + \Phi_1)}{|x + iv_0 t|^{\theta_0/4}|x + iv_{-1}t|^{1/(1+s)}} + A_2 \frac{\cos(4k_f x + \Phi_2)}{|x + iv_0 t|^{\theta_0}}$$
$$+ A_3 \frac{x^2 - (v_0 t)^2}{[x^2 + (v_0 t)^2]^2} + A_4 \frac{x^2 - (v_{-1}t)^2}{[x^2 + (v_{-1}t)^2]^2}, \quad (4.38)$$

and since the selection rules for the density-density correlator are identical to the selection rules for the longitudinal spin-spin correlator, the above calculation holds for C_σ^z with different constants and the replacement of $\mathcal{M}^2$ for n_0^2. Finally, for the transverse spin-spin and the single-particle correlator we find

$$C_\sigma^\perp(x, t) \quad \sim \quad A_0 \frac{\cos(2k_f x + \Phi)}{|x + iv_0 t|^{\theta_0/4}|x + iv_{-1}t|^{(1+s)}}$$
$$+ \frac{1}{|x + iv_{-1}t|^{2 + s^2/(1+s)}}\mathrm{Re}\left[A_1 \frac{x + iv_{-1}t}{x - iv_{-1}t}\right], \quad (4.39)$$
$$C_{sing}(x, t) \quad \sim \quad A_0 \frac{1}{|x + iv_0 t|^{4/\theta_0}|x + iv_{-1}t|^{1/(1+s)}}$$
$$+ \frac{1}{|x + iv_0 t|^{4/\theta_0 + \theta_0/4}}\mathrm{Re}\left[A_1 e^{-i2k_f x}\frac{x + iv_0 t}{x - iv_0 t}\right]. \quad (4.40)$$

Following Equation (4.27), we calculate ξ_0 from the Fermi velocity v_0. In Figure (4.2), we plot the lines of constant ξ_0 in the (d_0, s) plane. Note that the value of $\theta_0(\xi_0)$ at zero density is given by 2(1), whereas for finite densities and vanishing interaction strength $s \rightarrow 0^-$, we have $\theta_0 \rightarrow 4$ ($\xi_0 \rightarrow \sqrt{2}$). As expected, this is the same behavior as in the Hubbard model for vanishing on-site interaction strength u. In particular, the explicitely s-dependent exponents in the SC model reduce to constant values as $s \rightarrow 0^-$ which are equal to the corresponding exponents in the Hubbard model. However, we can not bound θ_0 between those two values as we could for the Hubbard model. In fact, θ_0 is larger than 4 and continues to increase for finite densities and increasing negative interaction strength $s \rightarrow -1^+$. A plot of θ_0 as a function of the density d_0 for different values of the interaction strength s is given in Figure (4.3).

For bose statistics, D_0 and D_{-1} are restricted to integer values. The correlators of diagonal operators, i.e., the density-density correlator C_n and the longitudinal spin-spin
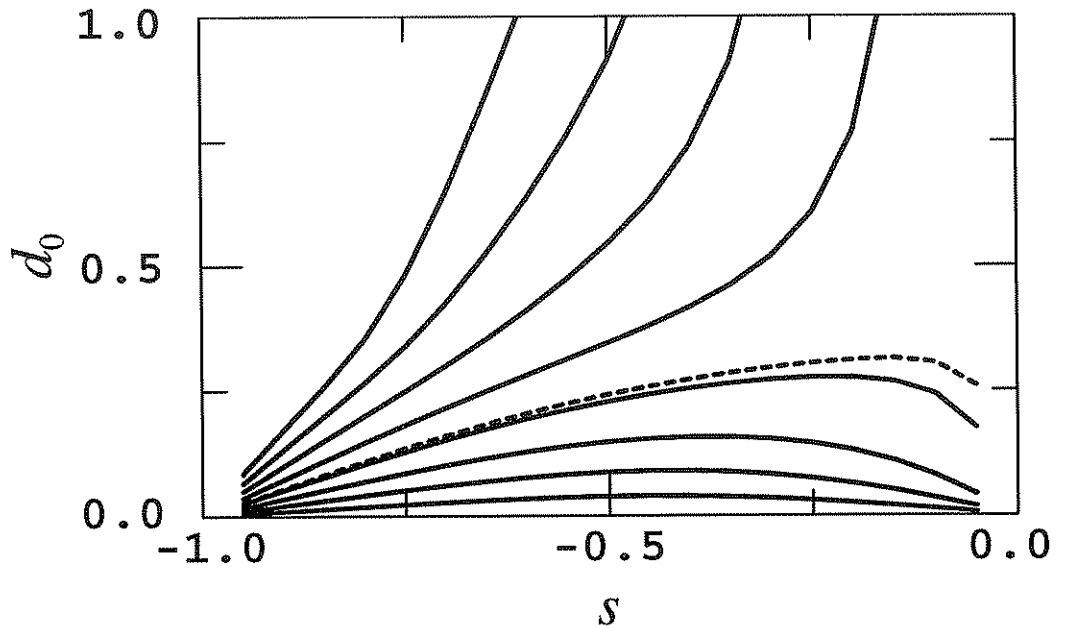
Figure 4.2. Lines of constant universal behavior for the unbound case. Contours of constant value of the dressed charge ξ_0 in the (d_0, s) plane are shown. The lines represent increments of .1 starting from $\xi_0 = 1.0$ at $d_0 = 0$ up to $\xi_0 = 1.8$. The dashed line correspond to the value $\xi_0 = \sqrt{2}$ of a noninteracting system.
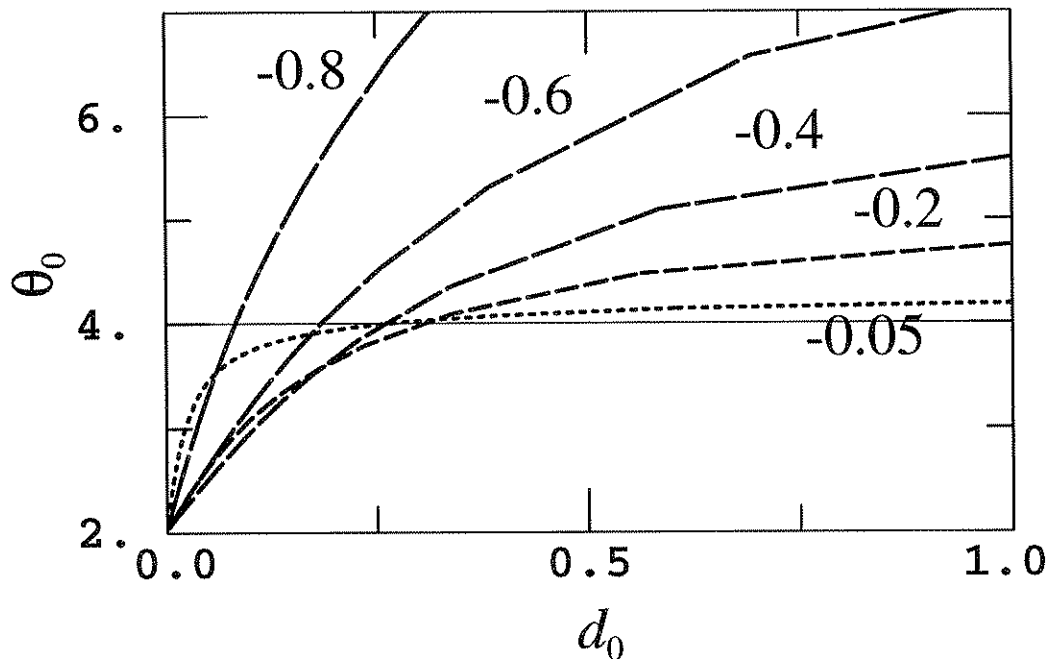
Figure 4.3. Plot of θ_0 as function of particle density d_0 for various values of interaction strength s for the unbound case.

correlator C_σ^z are independent of statistics, and so only the correlators C_ψ, $C_\sigma^\perp$ and C_{sing} change. We find for their asymptotics

$$
\begin{aligned}
C_\phi(x,t) &\sim A_0 \frac{1}{|x+iv_0t|^{1/\theta_0}|x+iv_{-1}t|^{(1+s)/4}} \\
&+ \frac{1}{|x+iv_0t|^{\theta_0/4+1/\theta_0}|x+iv_{-1}t|^{(s^2+4s+10)/8(1+s)}} \\
&\times \operatorname{Re}\left[A_1 e^{-i2k_f x}\left(\frac{x+iv_0t}{x-iv_0t}\right)^{1/2}\left(\frac{x+iv_{-1}t}{x-iv_{-1}t}\right)^{1/2}\right],
\end{aligned}
\tag{4.41}
$$

$$
\begin{aligned}
C_\sigma^\perp(x,t) &\sim A_0 \frac{1}{|x+iv_{-1}t|^{(1+s)}} \\
&+ \frac{1}{|x+iv_0t|^{\theta_0/4}|x+iv_{-1}t|^{2+s^2/(1+s)}} \\
&\times \operatorname{Re}\left[A_1 e^{-i2k_f x}\left(\frac{x+iv_{-1}t}{x-iv_{-1}t}\right)\right],
\end{aligned}
\tag{4.42}
$$

$$
\begin{aligned}
C_{sing}(x,t) &\sim A_0 \frac{1}{|x+v_0t|^{4/\theta_0}} \\
&+ \frac{1}{|x+iv_0t|^{\theta_0/4+4/\theta_0}|x+iv_{-1}t|^{1/(1+s)}} \\
&\times \operatorname{Re}\left[A_1 e^{-i2k_f x}\left(\frac{x+iv_0t}{x-iv_0t}\right)\right].
\end{aligned}
\tag{4.43}
$$

4.4 Asymptotic Correlation Functions for the Bound Case

4.4.1 The Dressed Charge Scalar

For the bound case in the zero sector, only the pair–pair-hole excitation branch is gapless. Thus there is only one excitation velocity and from the above arguments, we expect the dimensions of the primary operators to obey the formulae for a single $c = 1$ Gaussian model, i.e.,

$$
\Delta^\pm(\Delta N_1, D_1) = \frac{1}{2}\left(D_1\xi_1 \pm \frac{\Delta N_1}{2\xi_1}\right)^2.
\tag{4.44}
$$

The coupling constant ξ_1 of this Gaussian model depends on the system parameters. It is called the *dressed charge scalar* and may be calculated from the Bethe-Ansatz equations by means of an integral equation [49]

$$
\xi_1(k) = 2 - \frac{1}{2\pi}\int_{-D}^{D} \xi_1(h)\theta'_{1,1}(h-k)\mathrm{d}h,
\tag{4.45}
$$

where the constant is 2 because this excitation is a pair. However, we can again calculate $\xi_1 \equiv \xi_1(D)$ by purely thermodynamical arguments as follows: Let us change a given ground state configuration by adding pairs while keeping the Fermi sea at zero momentum,

so that the excitation can be described by $(\Delta N_1, D_1 = 0)$. Then a second order expansion gives

$$\Delta E = -\mu_1 (\Delta N_1) + \frac{1}{2} \frac{1}{L \kappa_1 d_1^2} (\Delta N_1)^2, \qquad (4.46)$$

where $\mu_1 = -\frac{\partial E}{\partial N_1}$ is the chemical potential for adding pairs and κ_1 is the pair-compressibility. Comparison with (4.1) and (4.44) yields

$$\xi_1^2 = \pi v_1 \kappa_1 d_1^2 = \pi d_1 / v_1. \qquad (4.47)$$

In the last equation, we have used the well known relation $v_1^2 = 1/(\kappa_1 d_1)$. Therefore, by knowing the Fermi velocity of the pair – pair-hole excitations, we can calculate the scaling dimensions.

4.4.2 Correlators

For $s > 0$, the model exhibits a gap for breaking of pairs and there are no spin waves. Therefore the correlators (4.28), (4.30) and (4.31) will decay exponentially. Let us introduce the pair field operator Ψ. The pair density - pair density correlator can be written in terms of the pair number operator $p = \Psi^\dagger \Psi$ as

$$C_p(x, t) = \langle p(x, t) p(0, 0) \rangle, \qquad (4.48)$$

and the pair field correlator is given by

$$C_\Psi(x, t) = \langle \Psi^\dagger(x, t) \Psi(0, 0) \rangle. \qquad (4.49)$$

As before, we can construct these correlators by an expansion in primary fields, minimizing with respect to ΔN_1 and D_1.

The pair quantum numbers H_j are restricted by the parity of N_1, and bose and fermi statistics are given as

$$H_j = (N_1 + 1)/2 \ (\text{mod } 1), \qquad (4.50)$$

since pair-pair scattering is symmetric for pairs of bosons and pairs of fermions. Due to these restriction on the quantum numbers of a given state, D_1 is an integer or half-odd integer depending on the parity of ΔN_1 for both bose and fermi statistics of the particles, i.e.,

$$D_1 = \frac{\Delta N_1}{2} \ (\text{mod } 1). \qquad (4.51)$$

This selection rule is just the same as the case of one component bosons, and so we find for the asymptotics of the pair density correlator

$$C_p(x, t) - d_1^2 \quad \sim \quad A_1 \frac{x^2 - (v_1 t)^2}{[x^2 + (v_1 t)^2]^2}$$

$$+ A_2 \cos(2k_f x + \varphi_1) \frac{1}{|x + iv_1 t|^{\theta_1}}, \tag{4.52}$$

and for the pair field correlator

$$\begin{aligned} C_\Psi(x,t) \quad \sim \quad & A_1 \frac{1}{|x + iv_1 t|^{1/\theta_1}} \\ & + \frac{1}{|x + iv_1 t|^{\theta_1 + 1/\theta_1}} \mathrm{Re} \left[A_2 e^{-i2k_f x} \frac{x + iv_1 t}{x - iv_1 t} \right]. \end{aligned} \tag{4.53}$$

Here we again defined an exponent $\theta_1 = 2\xi_1^2$. Following Equation (4.47), we can calculate ξ_1 from the Fermi velocity of pairs v_1. In Figure (4.4), we plot the lines of constant ξ_1 in the (d_0, s) plane. Note that the value of $\theta_1(\xi_1)$ at zero density is given by 8(2), whereas for finite densities and vanishing interaction strength $s \to 0^+$, we have $\theta_1 \to 4$ ($\xi_1 \to \sqrt{2}$). A plot of ξ_1 as a function of the density d_0 for different values of the interaction strength s is given in Figure (4.5).

4.5 The Noninteracting Two-Component System

At $s = 0$, the system reduces to a noninteracting two-component gas and we may expect a certain continuity in the behavior of the correlators at this point. Indeed, as $s \to 0^-$, the two Fermi velocities v_0 and v_{-1} both approach the Fermi velocity of a non-interacting single-component model, i.e., $v_0(s \to 0^-) = \pi d_0/2 = \pi d_{-1} = v_{-1}(s \to 0^-)$, as shown in Chapter 3. Consequently, the correlation functions of the bosonic (fermionic) system reduce to the correlation functions of a noninteracting bose (fermi) system with two components, i.e., with half the one component fermi momentum. Using the language of conformal field theory, we can thus describe the excitations of the noninteracting two-component gas by a $c = 2$ generalized Gaussian model [49].

From the expression of the dressed charges ξ_0 and ξ_1, we see that $\xi_1^2 = \frac{1}{2}\xi_0^2 \frac{v_0}{v_1}$. As $s \to 0^+$, the Fermi velocity of the pairs goes to the Fermi velocity of a one component free bose gas with doubled particle mass, i.e., $v_1(s \to 0^+) = \pi d_1/2 = \frac{1}{2}v_0(s \to 0^-)$. Therefore, we expect $\theta_1 = \theta_0$ at $s = 0$ and this is indeed true as shown above. Furthermore, the free energy of the system should be uniquely specified at $s = 0$. Following (4.7) we may write the finite temperature corrections for the unbound case as

$$F(T) \simeq F(T = 0) - \frac{\pi T^2}{6} \left(\frac{1}{v_{-1}} + \frac{1}{v_0} \right), \tag{4.54}$$

whereas for the bound case we have

$$F(T) \simeq F(T = 0) - \frac{\pi T^2}{6 v_1}. \tag{4.55}$$
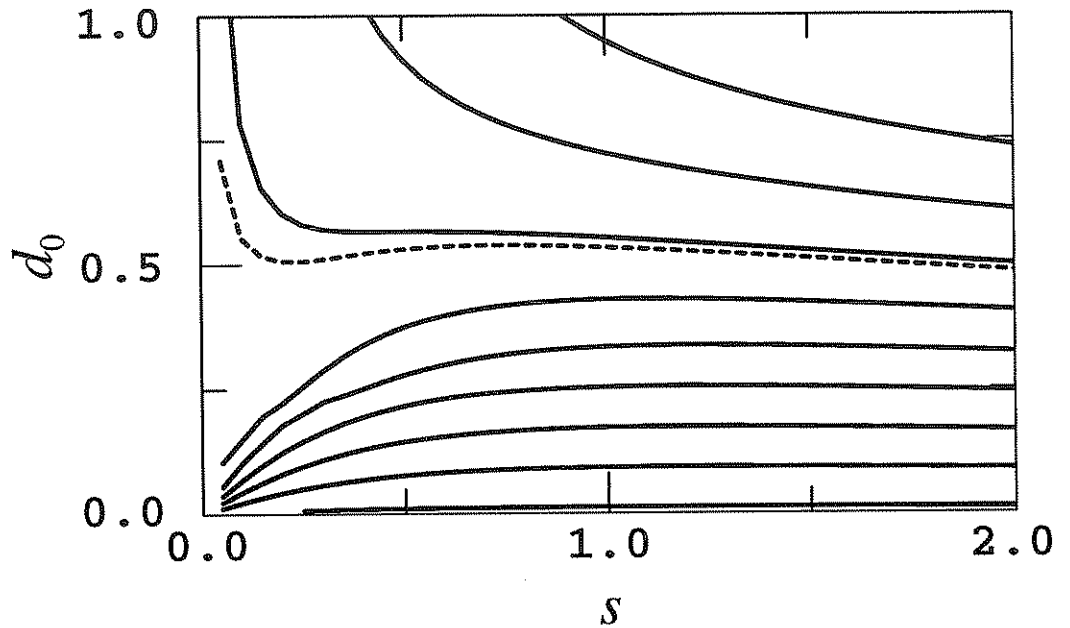
Figure 4.4. Lines of constant universal behavior for the bound case. Contours of constant value of the dressed charge ξ_1 in the (d_0, s) plane are shown. The lines represent increments of .1 starting from $\xi_1 = 2.0$ at $d_0 = 0$ down to $\xi_1 = 1.2$. The dashed line correspond to the value $\xi_1 = \sqrt{2}$ of a noninteracting system.
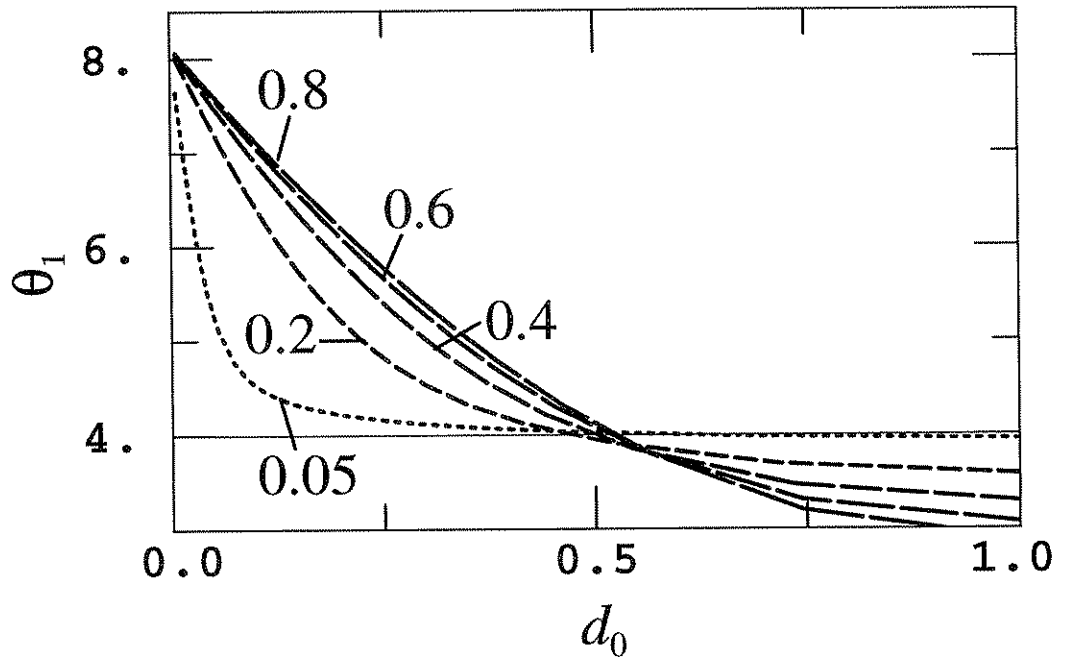
Figure 4.5. Plot of θ_1 as function of particle density d_0 for various values of interaction strength s for the bound case.

As predicted, these two equations are in agreement at $s = 0$ and identical to the free energy of a noninteracting $c = 2$ system.

The bound pairs for $s > 0$ are singlets. Therefore we might expect that the pair field correlator (4.49) becomes identical to the singlet pair correlators (4.32) and (4.43) of the unbound case as $s \to 0$. However, $\Psi^\dagger$ creates pairs with characteristic length scale $1/s$ and not just two particle wave functions. Thus, the pair wave functions include a normalization factor $\sqrt{s}$. As $s \to 0^+$, the leading terms of the conformal expansion (4.53) consequently vanish and higher order terms become important. It should therefore come as no surprise that the expansions (4.32), (4.43) and (4.53) do not agree at $s = 0$.

CHAPTER 5

TRANSPORT PROPERTIES OF THE UNBOUND CASE

In this chapter, we will further explore the connection of the SC model with the H-I model by examining the response of the system to a flux Φ. The addition of a flux is compatible with integrability and allows the study of the transport properties by an adiabatic variation of Φ. For the H-I model, this has already been done [68, 69, 70] for the interaction strength range $-1 \leq \Delta \leq 1$. We will show that the spin degrees of freedom of the SC model for $-1 < s < 0$ may be usefully viewed as a H-I model with moving H-I spins. The presence of the translational degrees of freedom will simply renormalize the spin-spin coupling.

5.1 The Twisted Bethe Ansatz Equations

We thus restrict ourselves in what follows to the unbound case $-1 < s < 0$, such that there are two gapless excitations corresponding to a particle-hole and a two spin-wave continuum with Fermi velocities v_0 and v_{-1}, respectively. Let us then modify the Bethe Ansatz Equations (3.1) by threading them with a flux Φ. We have two coupled equations for N_0 particles with pseudo-momenta $\mathbf{k} = (k_1, \ldots, k_{N_0})$ and N_{-1} spin waves with rapidities $\boldsymbol{\lambda} = (\lambda_1, \ldots, \lambda_{N_{-1}})$ on a ring of length L. The energy of a given state is $E(\mathbf{k}) = \frac{1}{2} \sum_{j=1}^{N_0} k_j^2$ and the total momentum is $P(\mathbf{k}) = \sum_{j=1}^{N_0} k_j$. Boosting the system by Φ will accelerate the two kinds of particles in opposite directions due to the two components being of equal but *opposite* charge. Therefore, we have no center-of-mass motion and $P = 0$. The energy of a given state will change as a function of Φ, and the energy shift of the ground state may be written as $\Delta E_0(\Phi) \equiv E_0(\Phi) - E_0(0) \equiv D\Phi^2/2L + O(\Phi^4)$, where D is called the *stiffness constant* and can be specified by perturbation arguments for Φ up to π [69]. Note that since we do not have any center-of-mass motion, we can call D either spin or charge stiffness depending on what interpretation of σ we adopt. We choose the spin language for comparison with the H-I model. However, the charge interpretation

is probably more natural to describe transport properties. We furthermore caution the reader that the term charge stiffness has been previously used in lattice models to describe center-of-mass motion.

The twisted Bethe Ansatz Equations (3.1) are given by

$$L k_j = 2\pi I_j(k_j) - \frac{N_{-1}}{N_0}\Phi + \sum_{a=1}^{N_{-1}} \theta_{0,-1}(k_j - \lambda_a) + \sum_{l=1}^{N_0} \theta_{0,0}(k_j - k_l), \qquad (5.1a)$$

$$0 = 2\pi J_a(\lambda_a) + \Phi + \sum_{b=1}^{N_{-1}} \theta_{-1,-1}(\lambda_a - \lambda_b) + \sum_{j=1}^{N_0} \theta_{0,-1}(\lambda_a - k_j). \qquad (5.1b)$$

The two-body phase shifts for particle-particle, particle-spin wave and spin wave-spin wave scattering, $\theta_{0,0}(k)$, $\theta_{0,-1}(k)$ and $\theta_{-1,-1}(k)$ respectively, have been given in Chapter 2. The particle quantum numbers I_j and the spin-wave quantum numbers J_a are integers or half-odd integers depending on the parities of N_0, N_{-1} as well as on the particle statistics as shown in the last chapter. For comparison with the H-I model, we use mostly bosonic selection rules, although a purely fermionic or a mixed bose-fermi system may be studied along similar lines.

We start with some general considerations. Let us denote by $E_{\{I,J\}}(\Phi)$ the energy of a state specified by the $\Phi = 0$ set of quantum numbers $\{I, J\}$. We then adiabatically turn on the flux until we return to our initial state. The energy will also return to its initial value, although, it may return sooner; so, the period of the wave function will be an integer multiple of the period of the energy. We can define a topological winding number n to be the number of times the flux Φ increases by 2π before the state returns to its initial value. As Sutherland and Shastry have shown, the ground state winding number of the H-I model with $S_z = 0$ in the parameter range $-1 < -\cos(\mu) \equiv \Delta < 1$ is 2, implying charge carriers with half the quantum of charge, *except* at isolated points $\Delta = \cos(\pi/Q)$, where $N_{-1} \geq Q \geq 2$ is an integer. In particular, at $\Delta = 0$, the free particle wave function has periodicity $2\pi N_{HI}$, where N_{HI} is the number of H-I sites, implying free acceleration in the thermodynamic limit.

We now note the following important fact: Choosing $\mu \equiv -\pi s$, the spin wave-spin wave phase shift $\theta_{-1,-1}$ is identical to the spin-spin phase shift in the H-I model. Using the same identification for the spin wave-particle phase shift $\theta_{0,-1}$ we may rewrite the equation for the rapidities as

$$N_0 \bar{\theta}_{0,-1}(\lambda_a, \mu) \equiv N_0 \sum_{j=1}^{N_0} \theta_{0,-1}(\lambda_a - k_j, \mu)/N_0 = 2\pi J_a(\lambda_a) + \Phi + \sum_{b=1}^{N_{-1}} \theta_{-1,-1}(\lambda_a - \lambda_b, \mu).$$
(5.2)

which nearly is identical to the Bethe Ansatz equation of the H-I model, as can be readily seen when we use the standard transformation for the H-I momenta

$$p = 2 \arctan[\tanh(\alpha/2)/\cot(\mu/2)].$$
(5.3)

We then merely have to identify $\alpha \equiv \pi\lambda$. The sole effect of the pseudo-momenta $\mathbf{k}$ is an averaging on the left hand side. We can furthermore define a *crystal momentum* $\mathcal{P}$ and write

$$\mathcal{P} \equiv \sum_{\lambda_a} \bar{\theta}_{0,-1}(\lambda_a, \mu).$$
(5.4)

$\mathcal{P}$ is the analogue of the momentum in the lattice gas picture of the H-I model [69] and we have $\mathcal{P} = N_{-1}\Phi/N_0$.

5.2   Stiffness and Susceptibility

Let us now restrict ourselves in what follows to the neutral (spin zero) sector such that we have N_{-1} particles with $\sigma = -1$ and N_{-1} particles with $\sigma = +1$ for a total of $N_0 = 2N_{-1}$. Then, a discussion of the behavior of the rapidities λ for varying Φ exactly mimics the discussion of the H-I momenta p in [69] at $S_z = 0$: As long as $|\Phi| \leq 2\pi(s+1)$, all λ's stay on the real axis. At $\Phi = 2\pi(s+1)$, the largest root $\lambda_{N_{-1}}$ goes to infinity. For Φ increasing beyond this point, $\lambda_{N_{-1}}$ will reappear from infinity as $i\pi + \gamma_1$ until exactly at $\Phi = 2\pi$, $\lambda_{N_{-1}} = i\pi$ ($\gamma_1 = 0$) and the remaining $N_{-1} - 1$ rapidities have redistributed themselves symmetrically around 0 on the real axis. The momenta $\mathbf{k}$ are always real and distributed about the origin. However, as mentioned above, this behavior is different at the threshold values $s = (1 - Q)/Q$. Eq.(5.1b) simplifies at $\Phi = 2\pi(s+1)$ (and thus $\lambda_{N_{-1}} = \infty$) and is in fact just the equation of $N_{-1} - 1$ rapidities in the ground state. So as in [69] using simple thermodynamical arguments, we may write

$$\Delta E_0(2\pi(s+1)) = E_0(N_0, N_{-1} - 1) - E_0(N_0, N_{-1}) = 1/2L \cdot \chi^{-1},$$
(5.5)

where χ is the susceptibility. Comparing with the definition of the stiffness constant D, we find

$$D = \chi^{-1}/4\pi^2(s+1)^2.$$
(5.6)

On the other hand, we can read off the finite-size energy corrections for the SC model, and then finite-size arguments of conformal field theory give an expression for $\Delta E_0(2\pi(s+$

1)) in terms of the conformal weights, the dressed charge matrix Ξ and the spin wave velocity v_{-1}. The neutral sector dressed charge matrix is given in Equation (4.18) and thus we have for $\Delta N_0 = 0$, $\Delta N_{-1} \neq 0$ and $\mathbf{D} = 0$,

$$\Delta E = \frac{\pi v_{-1}(s+1)}{L}(\Delta N_{-1})^2.$$

The susceptibility is defined as $\Delta E \simeq \frac{1}{2L\chi}(\Delta N_{-1})^2$ and therefore, we have

$$\chi^{-1} = 2\pi v_{-1}(s+1). \tag{5.7}$$

By comparison with Equation (5.6), we may then express the stiffness D in terms of the spin wave velocity as

$$D = v_{-1}/2\pi(s+1). \tag{5.8}$$

We emphasize that this formula for D is true also for a system of purely fermionic particles. Shastry and Sutherland [69] have given an exact formula for the stiffness constant in the H-I model, by using the known expression for the H-I model spin wave velocity $v_{-1} = \pi \sin(\mu)/\mu$ [71, 72]. No such expression is known for the SC model and we can only give v_{-1} as in Equation (3.30). However, written in terms of spin velocities the stiffness formulas are identical and only the values of the respective spin wave velocities are different. Thus the presence of the translational degrees of freedom in the SC model simply renormalizes the spin-wave velocity.

Note that Equation (5.8) may also be written as

$$D\chi^{-1} = v_{-1}^2. \tag{5.9}$$

This is nothing but the analogue of the well-known hydrodynamical relation between compressibility and velocity of sound waves. Let us briefly explain how to derive this formula without having to use arguments of conformal field theory.

Given a gapless excitation branch, we know that long wave length hydrodynamical fluctuations are important and we can define thermodynamical quantities such as compressibility and stiffness. Then, since the particle number is conserved, there is a continuity equation and so also a wave equation for the excitations. By standard thermodynamical arguments [73], we can now immediately read off Equation (5.9). However, we have to treat the flux Φ as a thermodynamical variable for this argument to be valid. A discussion of this and related points can be found in [74, 75]. We emphasize, that the arguments are quite general for all one-dimensional quantum models with gapless excitations.

5.3 Iteration

We have iterated the Bethe Ansatz Equations (5.1) in the neutral sector for reasonably large systems and density $d \equiv N_0/L = 1/2$ as a function of Φ. By our correspondence between the H-I model, and the spin wave part of the SC model, we expect *free spin waves* at $s = -1/2$. In the thermodynamic limit, we would thus expect the periodicity of the ground state energy to be infinite. For a finite system, this will be reduced to a periodicity that scales with the system size. For the SC model we have indeed found that at $s = -1/2$ the periodicity of the ground state energy is given as $2\pi N_0$. Note that the winding number is N_0, the number of particles, and not L, the number of sites. This again confirms that the SC model for $-1 < s < 0$ may be viewed as a H-I model with N_0 moving H-I sites (SC particles) on a ring of length L. We may then speak of $s \to -1^+$ as the ferromagnetic critical point and $s \to 0^-$ as the antiferromagnetic critical point of the SC model.

In Figure (5.1), we show the full spectrum of low-lying states with zero momentum corresponding to bosonic particle statistics, respectively, at interaction strength $s = -1/2$ for $L = 12$, $N_0 = 6$ and $N_{-1} = 3$. The ground state curve is emphasized and its periodicity is $6 \cdot 2\pi$. Figure (5.2) shows the behavior of the pseudo-momenta $\mathbf{k}$ and the real and complex rapidities λ and γ for the ground state Ψ_0. The behavior of $\mathbf{k}$, λ and γ for the state Ψ_1 is obtained by shifting the origin of Figure (5.2) by $\Delta\Phi = 4\pi$ to the right. We emphasize that in this free spin wave case the behavior of the rapidities as functions of the flux Φ is different from the behavior discussed in the last section. In particular, as we increase the flux, the rapidities go complex one after the other, until at $\Phi = \pi N_0$, i.e., half the period, *all* will have reappeared as γ's.

Note that at $\Phi = 2\pi$ there is a level crossing between ground state and first exited state in Figure (5.1). When the interaction strength changes from $s = -1/2$, immediately a gap opens between the ground state and first exited state. Just as in the H-I model the periodicity is reduced to 4π. Note that a perturbation theory argument can not describe this behavior. Figure (5.3) shows the behavior of the ground state energy variation $L[1 - E(\Phi)/E(2\pi)]$ for $s = -1/3$ near $\Phi = 2\pi$ for different lattice sizes. The rounding is well pronounced and does not vanish as we increase the size.

Thus the behavior of the low-lying states in the SC and H-I models are qualitatively the same, up to the renormalization of quantities such as the spin wave velocity v_{-1}. Let us briefly describe the behavior of the gaps in the H-I model, keeping in mind the

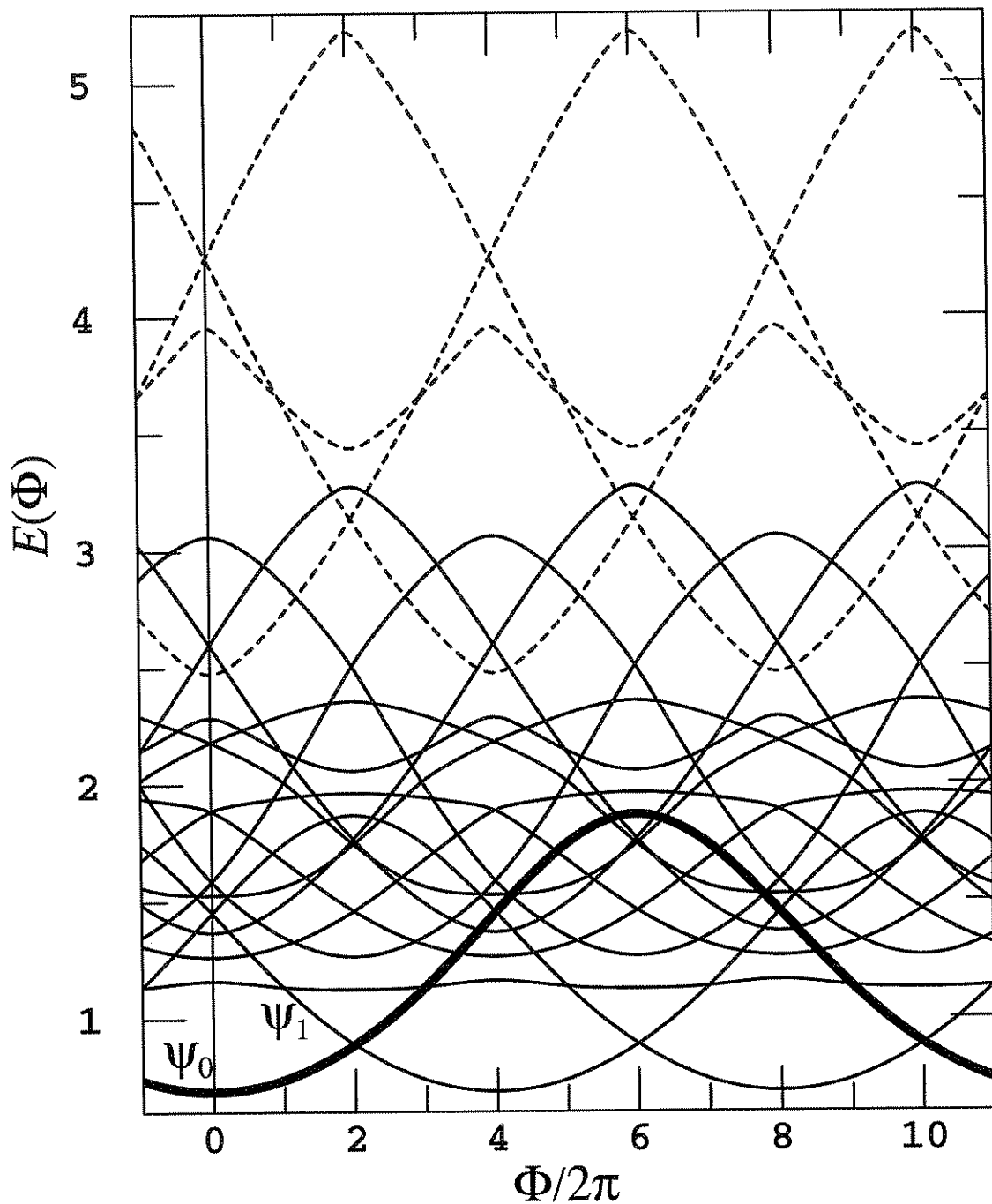**Figure 5.1.** The low-lying states for the bosonic SC model at $L = 12$, $N_0 = 6$ and $N_{-1} = 3$. The bold curve corresponds to the ground state Ψ_0. The winding number of Ψ_0 is $n = 6 = N_0$. Note the various level crossing in this free spin wave case, especially the crossing of Ψ_0 and the first exited state Ψ_1 at $\Phi = 2\pi$. The dashed curves correspond to four higher lying states.
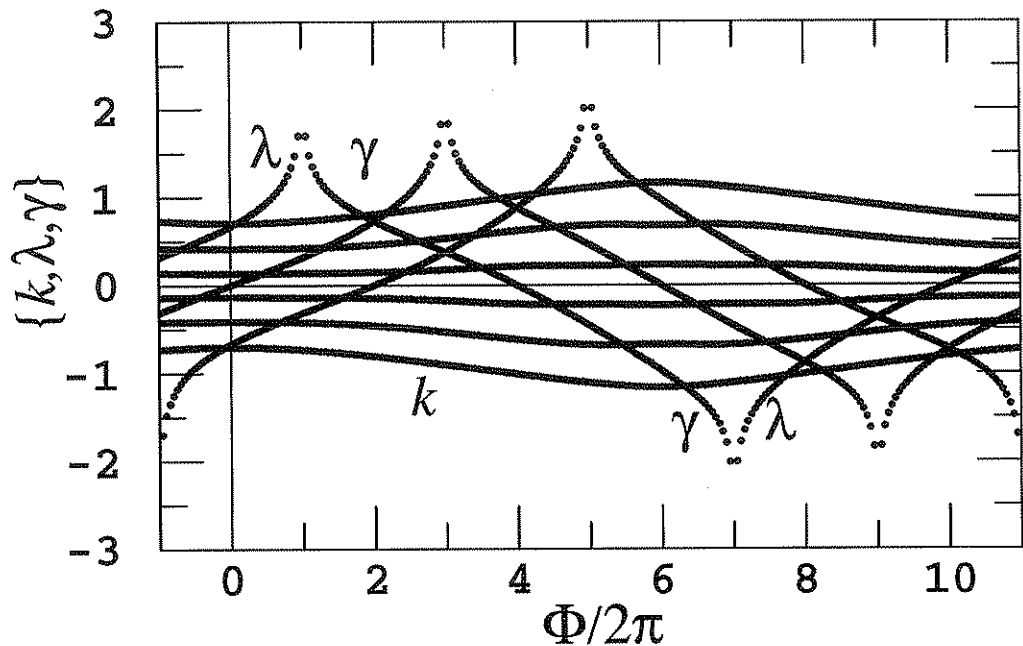
Figure 5.2. Pseudo-momenta **k**, rapidities λ and complex rapidities γ as a function of flux Φ for the ground state Ψ_0 of the bosonic SC model at $s = -1/2$, $L = 12$, $N_0 = 6$ and $N_{-1} = 3$. The initial quantum numbers for this state are **I** $= \{-5/2, -3/2, -1/2, 1/2, 3/2, 5/2\}$ and **J** $= \{-1, 0, 1\}$. Note the periodicity of $2\pi N_0$ for the λ/γ cycle and the symmetry of the pseudo-momenta **k** around 0.

Figure 5.3. Plot of the ground state energy variation $L[1 - E(\Phi)/E(2\pi)]$ for the SC model at $s = -1/3$ for $L = 12, 20$ and 28.

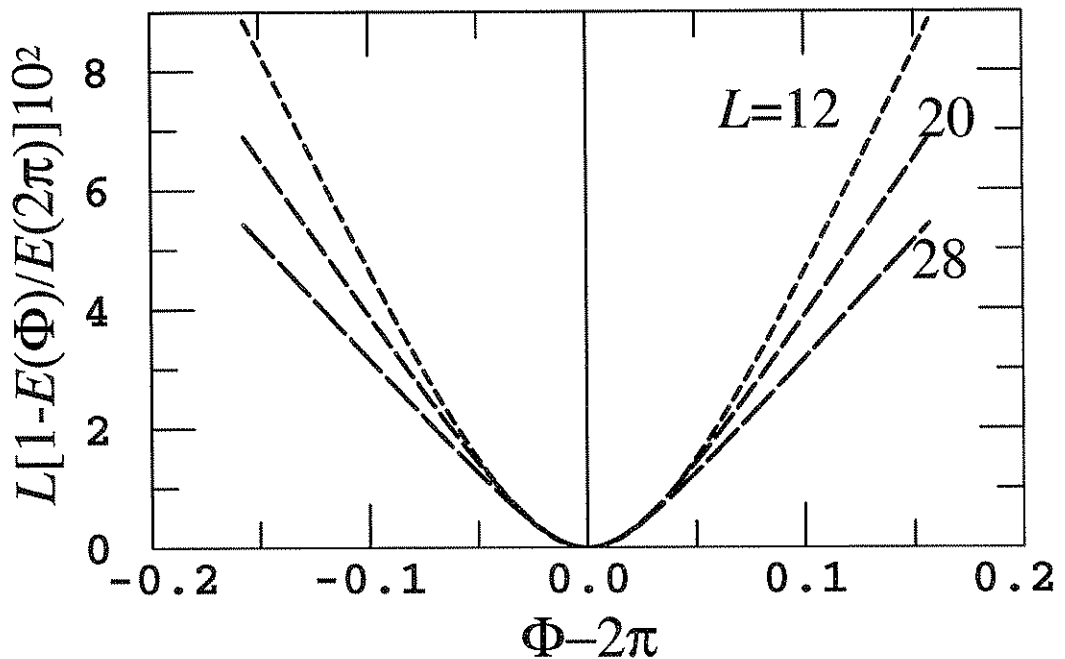correspondence $\mu = -\pi s$. Increasing μ beyond $\pi/2$ ($\Delta = 0$), we see that the gap continues to widen up to a maximum value at $\mu \sim 7\pi/12$ ($\Delta \sim 0.26$). It then closes up again exactly at $\mu = 2\pi/3$ ($\Delta = 1/2$). As has been noted before, this value of μ coincides with the appearance of a $Q = 3$ string [13]. Further increase of μ again opens, and then closes the gap at the threshold for the next-longer $Q = 4$ string. This behavior continues, and the threshold values accumulate as $\mu \to \pi$ ($\Delta \to 1$). In Figure (5.4), we show the ground state and the first exited state of the H-I model on a ring of $N_{HI} = 12$. Note that due to the finite size of the ring, we can only observe strings up to length $Q = 6$. We will present a more detailed finite-size study of the behavior of the gaps in H-I and SC model in another publication. We only mention that for fixed μ the gap scales with the system size as a power, with variable exponent depending on the coupling constant μ.

The stiffness constant D can be read off from the curvature of the ground state energy $E_0(\Phi)$ as a function of Φ. In Figure (5.5), we show D for systems of 12, 24 and 32 lattice sites. We also show the behavior of D as given by Eq.(5.8). As $s \to 0^-$, the spin wave velocity approaches the velocity of a noninteracting single-component model, i.e., $v_{-1} \to \pi d/2$, as shown in Chapter 3. Thus D approaches the nonzero value $1/8$ which is compatible with the result of [69]. Furthermore, the SC model exhibits a gap for $s > 0$ and so D is zero. Thus D exhibits a jump discontinuity at $s = 0$ just as in the H-I model for $\Delta = -1$.

The derivation of the hydrodynamical relation is valid in the thermodynamical limit by construction. Most of the other results given above have been derived using Equation (5.1). These equations, however, have been derived by the asymptotic Bethe Ansatz. This method is only correct in the thermodynamic limit [17]. Indeed the finite-size formula for the energy of the periodic $1/r^2$ model derived from the asymptotic Bethe Ansatz is incorrect and only as $L \to \infty$, d constant, does one recover the correct result [20]. Thus all our finite-size results should exhibit correction terms. From the hyperbolic form of the pair potential (1.3), we may expect these corrections to be exponentially small in L. Indeed, the log-log plot of the ground state energy versus L at fixed interaction strength is given in Figure (5.6) and shows a simple power law behavior already for $L \geq 6$. Thus the $L \to \infty$ behavior of the finite-size Bethe-Ansatz equations for the SC model does not seem to differ in any significant respect from usual finite size behavior for short ranged models. This further supports our use of the asymptotic Bethe Ansatz in the present study.
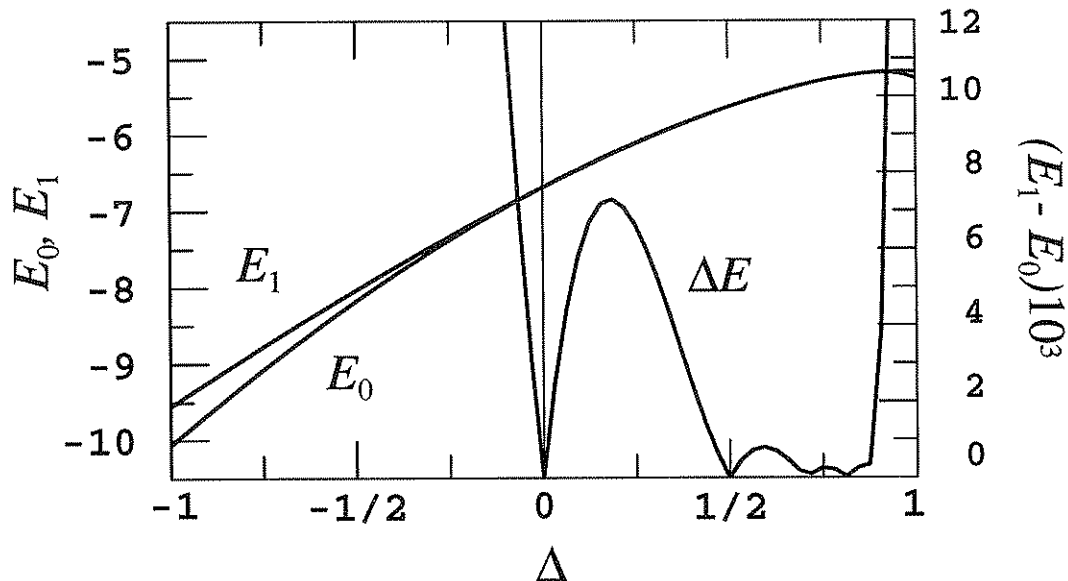
Figure 5.4. Energy of the ground state and first exited state and their difference in the H-I model at $\Phi = 2\pi$ for $N_{HI} = 12$. Note the closing of the gap at $\Delta = \cos(\pi/Q)$ for $Q = 2, 3, 4, 5$.
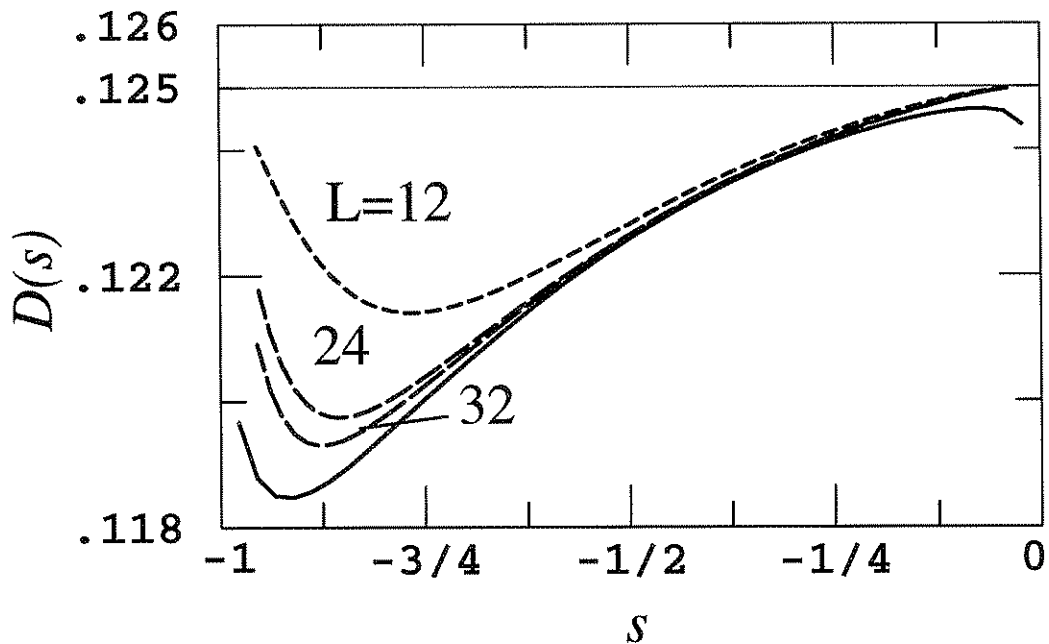
Figure 5.5. The charge stiffness $D(s)$ for the SC model. The dashed curves correspond to $L = 12$, 24 and 32 and converge to $D(0) = 1/8$ at $s \to 0^-$. The solid curve comes from Equation (5.8), which can be derived by conformal methods or from thermodynamics. (Note that as $s \to 0^-$, the solid curve does not converge to 1/8. This is due to a buildup of numerical errors in the integration routine.)

Figure 5.6. Log-log plot of E_0 versus L for values of $s = -0.04, -0.22, -0.40, -0.57, -0.75$ and -0.93 corresponding to increasing dash length. For $L > 10$, we see straight lines corresponding to purely algebraic finite-size behavior.

CHAPTER 6

CONCLUSIONS

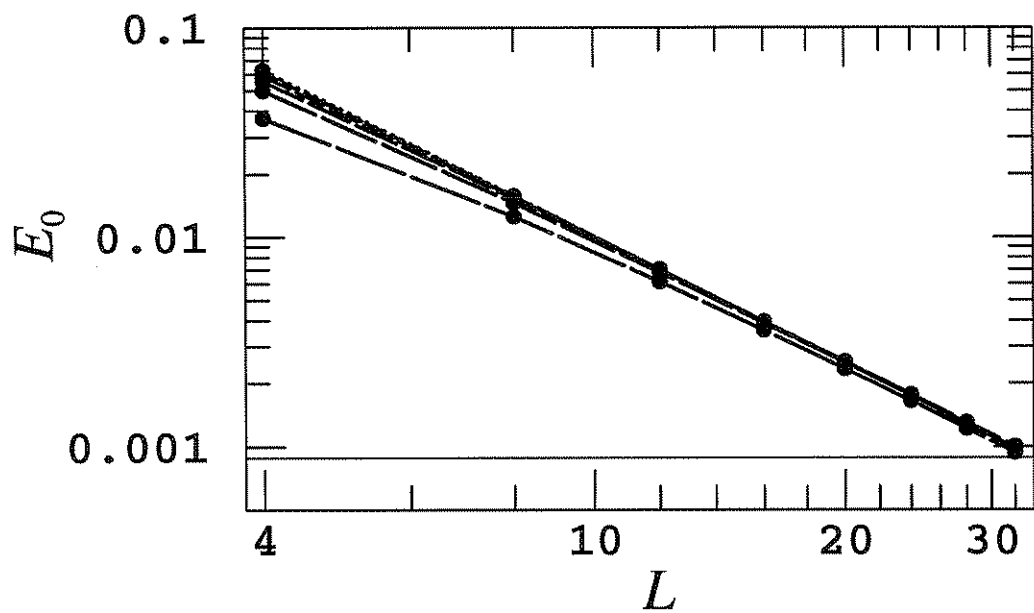In the preceding chapters, we introduced the SC model as a one-dimensional two-component quantum many-body system with competing interactions. We subsequently proceeded to solve the model exactly in the thermodynamic limit and computed the asymptotic behavior of the correlation functions. Finally, we threaded the system with a flux and calculated the stiffness and the susceptibility.

The physics of the SC model is surprisingly rich. For $-1 < s < 0$, where there are no bound states, we showed that there is a close relationship to the Heisenberg-Ising model. Indeed, we argued that the SC model may be usefully viewed as Heisenberg-Ising fluid with moving spins. This then would open the possibility of modeling magnetic systems in which the magnetic centers are moving themselves. A corresponding behavior had not been seen previously in other models. However, we may also interpret the quantum number σ as charge and the connection with the H-I model becomes purely formal.

For $s > 0$, we have an even richer structure due to the presence of exciton-like excitations. Previous attempts to incorporate excitons in exactly-solvable models such as the Hubbard model had been unsuccessful, since necessary additional interaction terms such as next-nearest neighbor interactions usually violate the integrability. Thus the SC model is the first exactly-soluble model with a natural description of exciton-like modes.

We applied finite-size scaling arguments of conformal field theory for the calculation of the *asymptotics* of various correlation functions. However, there has recently been a breakthrough regarding the calculation of the *exact* correlation functions for the $1/r^2$ model [76] and the reader may wonder whether we could have done the same for the SC model. The calculation of correlation functions in the $1/r^2$ model makes use of the close relation of the ground state wave function and the level distribution of eigenvalues of random matrices [77, 78]. Unfortunately, there is no such relation for the SC model and we can do no better than calculate the asymptotics via conformal arguments.

We have used quite general arguments to show that the universality class of one-dimensional quantum systems with gapless excitations is given by the $c = 1$ Luttinger model. These arguments are — to the best of our knowledge — confirmed in all one-dimensional models with short-range interactions. In long-ranged models, one can no longer simply read off c from Equation (4.6) and the plot (4.1) of c versus s shows a varying $c(s) \leq 1$ for $-1 < s < 0$. Excluding the unphysical possibility of a continuously varying universality class, this then must be wrong: In chapter 5, we show that the susceptibility (5.7) varies with s using arguments independent of conformal finite-size scaling. However, the susceptibility is closely connected with the conformal weights for any c [79]. Therefore, we can expect the conformal weights to vary with s, too. This then has been shown to be allowed behavior for universality classes of $c \geq 1$ only, since for $c < 1$ the Kac formula uniquely specifies the weights already. Moreover, it has been argued that continuously varying weights are most naturally described with a $c = 1$ theory. We therefore conclude that the universality class of the SC model is indeed $c = 1$. However, more work is needed to explain the failure of Equation (4.6) and we are currently involved in a study of this question along the ideas outlined in section 4.2. Let us close this brief discussion by noting that, as shown in Chapter 4, the low temperature corrections to the free energy as in Equation (4.7) seem to be correct.

We have restricted ourselves in this dissertation to the zero sector of the SC model at zero temperature. Studies of finite-temperature properties and of the full phase diagram away from the zero sector are certainly very important especially regarding the possible comparison of the SC model to experimental results in low-dimensional systems. We hope to have the time to come back to these problems in the future.

REFERENCES

[1] J. G. Bednorz and K. A. Müller, Z. Phys. B **64**, 189 (1986).

[2] K. von Klitzing, G. Dorda, and M. Pepper, Phys. Rev. Lett. **45**, 494 (1980).

[3] D. C. Tsui, H. L. Störmer, and A. C. Gossard, Phys. Rev. Lett. **48**, 1559 (1982).

[4] H. Bethe, Z. Phys. **71**, 205 (1931).

[5] E. H. Lieb and W. Liniger, Phys. Rev. **130**, 1605 (1963).

[6] E. H. Lieb, Phys. Rev. **130**, 1616 (1963).

[7] J. B. McGuire, J. Math. Phys. **5**, 622, (1964).

[8] C. N. Yang, Phys. Rev. Lett. **19**, 1312 (1967).

[9] C. N. Yang, Phys. Rev. **168**, 1920 (1968).

[10] C. N. Yang and C. P. Yang, J. Math. Phys. **10**, 1115 (1969).

[11] L. Hulthén, Arkiv. Mat. Astron. Fysik **26A**, No. 11 (1938).

[12] J. C. Bonner and M. E. Fisher, Phys. Rev. **135**, A640 (1964).

[13] C. N. Yang and C. P. Yang, Phys. Rev. **150**, 321 (1966); **150**, 327 (1966).

[14] E. H. Lieb and F. Y. Wu, Phys. Rev. Lett. **20**, 1445, (1968).

[15] C. N. Yang, Phys. Rev. Lett. **19**, 1312 (1967); Phys. Rev. **168**, 1920 (1968).

[16] R. J. Baxter, Phys. Rev. Lett. **26**, 832 (1971); Ann. Phys. (N.Y.) **70**, 193 (1972); *Exactly Solved Models in Statistical Mechanics* (Academic, London, 1982).

[17] B. Sutherland, in *Festschrift Volume for C.N. Yang's 70th Birthday*, edited by S.T. Yau (International, Hong Kong, in press).

[18] D. Haldane, Phys. Rev. Lett. **67**, 937 (1991).

[19] Y.-S. Wu, University of Utah preprint, 1994 (to be published).

[20] B. Sutherland, J. Math. Phys. **12**, 246 (1971); **12**, 251 (1971); Phys. Rev. A 4, 2019, (1971); **5**, 1372, (1972).

[21] R. B. Laughlin, Phys. Rev. Lett. **50**, 1395 (1983).

[22] B. S. Shastry, in *Proceedings of the 16th Taniguchi Symposium on the Theory of Condensed Matter: Correlation Effects in Low Dimensional Electron Systems*, edited by N. Kawakami and A. Okiji, (Springer Verlag, Tokyo, 1994).

[23] D. Haldane, Phys. Rev. Lett. **60**, 635 (1988).

[24] B. S. Shastry, Phys. Rev. Lett. **60**, 639 (1988).

[25] V. G. Drinfel'd, Dokl. Acad. Nauk. USSR **283**, 1060 (1985) [Sov. Math. Dokl. **32**, 254 (1985)].

[26] L. D. Landau and E. M. Lifschitz, *Lehrbuch der Theoretischen Physik* (Akademie Verlag, Leipzig, 1988), Band III, 8. Auflage.

[27] F. Calogero, O. Ragnisco, and C. Marchioro, Lett. Nuovo Cimento **13**, 383 (1975).

[28] B. Sutherland, Rocky Mtn. J. Math. **8**, 413 (1978).

[29] B. Sutherland, in *Exactly Solvable Probs in Condensed Matter and Relativistic Field Theory, Panchgani, India, 1985*, edited by B. S. Shastry, S. S. Jha and V. Singh (Springer, Berlin, 1985).

[30] P. D. Lax, Commun. Pure Appl. Math. **21**, 467 (1968).

[31] J. Moser, Adv. Math. **16**, 197 (1975).

[32] F. Calogero, Lett. Nuovo Cimento **13**, 411 (1975).

[33] B. S. Shastry and B. Sutherland, Phys. Rev. Lett. **70**, 4029 (1993).

[34] Abramowitz and I. A. Stegun, *Handbook of Mathematical Functions With Formulas, Graphs, and Mathematical Tables*, (National Bureau of Standards, Applied Mathematics Series 55, 1964).

[35] C. N. Yang, Phys. Rev. Lett. **19**, 1312 (1967).

[36] R. J. Baxter, *Exactly Solved Models in Statistical Mechanics* (Academic, London, 1982).

[37] B. S. Shastry, S. S. Jha and V. Singh, ed., *Exactly Solvable Problems in Condensed Matter and Relativistic Field Theory* (Springer, Berlin, 1985).

[38] B. Sutherland, (unpublished).

[39] F. D. M. Haldane, Phys. Rev. Lett. **66**, 1529 (1991).

[40] B. Sutherland and B. S. Shastry, Phys. Rev. Lett. **71**, 5 (1993).

[41] B. Sutherland and R. A. Römer, Phys. Rev. Lett. **71**, 2789 (1993).

[42] A. M. Polyakov, Zh. Eksp. Teor. Fiz. Pis. Red. **12**, 538 (1970) [Sov. Phys. JETP Lett. **12**, 381 (1970)].

[43] A. A. Belavin, A. M. Polyakov, and A. B. Zamolodchikov, Nuc. Phys. B **241**, 333 (1984).

[44] D. Friedan, Z. Qui, and S. Shenker, Phys. Rev. Lett. **52**, 1575 (1984).

[45] S. Tomonaga, Progr. Theoret. Phys. (Kyoto) **5**, 544 (1950).

[46] J. M. Luttinger, J. Math. Phys. **4**, 1154 (1963).

[47] D. C. Mattis and E. H. Lieb, J. Math. Phys. **6**, 304 (1965).

[48] F. D. M. Haldane, Phys. Rev. Lett. **45**, 1358 (1980); **47**, 1840 (1980); Phys. Letters **81** A, 153 (1981); J. Phys. C **14**, 2585 (1981).

[49] F. Woynarovich, J. Phys. A **22**, 4243 (1989).

[50] A. G. Izergin, V. E. Korepin and N. Yu Reshetikhin, J. Phys. A **22**, 2615 (1989).

[51] H. J. Schulz, Phys. Rev. Lett. **64**, 2831 (1990).

[52] N. Kawakami and S.-K. Yang, Phys. Lett. A **148**, 359 (1990).

[53] H. Frahm and V. E. Korepin, Phys. Rev. B **42**, 10553 (1990); **43**, 5653 (1991).

[54] E. B. Kolomeisky, (unpublished).

[55] A. D. Mironov and A. V. Zabrodin, Phys. Rev. Lett. **66**, 534 (1991).

[56] N. Kawakami and S.-K. Yang, Phys. Rev. Lett. **67**, 2493 (1991).

[57] R. A. Römer and B. Sutherland, Phys. Rev. B **48**, 6058 (1993).

[58] I. Affleck, Phys. Rev. Lett. **56**, 746 (1986).

[59] H. W. J. Blöte, J. L. Cardy, and M. P. Nightingale, Phys. Rev. Lett. **56**, 742 (1986).

[60] H. Frahm and A. Schadschneider, J. Phys. A **26**, 1463 (1993).

[61] F. Woynarovich and H.-P. Eckle, J. Phys. A **20**, L97 (1987).

[62] G. Gómez-Santos, Phys. Rev. Lett. **70**, 3780 (1993).

[63] K. B. Efetov and A. I. Larkin, Zh. Eksp. Teor. Fiz. **69**, 764 (1975) [Sov. Phys. JETP Lett. **42**, 390 (1976)].

[64] E. Fradkin and L. Susskind, Physical Review D **17**, 2637 (1978).

[65] J. B. Kogut, Rev. Mod. Phys. **51**, 659 (1979).

[66] J. L. Cardy, Nuc. Phys. B **270** [FS16], 186 (1986); J. Phys. A **20**, L891 (1987); *Conformal Invariance* in *Phase Transitions and Critical Phenomena*, eds. C. Domb, J. L. Lebowitz, vol. **11**, Academic Press (1987).

[67] R. A. Römer and B. Sutherland, Phys. Rev. B **49**, 6779 (1994).

[68] N. Beyers and C. N. Yang, Phys. Rev. Lett. **7**, 46 (1961).

[69] B. Sriram Shastry and B. Sutherland, Phys. Rev. Lett. **65**, 243 (1990); B. Sutherland and B. Sriram Shastry, *ibid.* **65**, 1833 (1990).

[70] N. Yu and Michael Fowler, University of Virginia preprint.

[71] C. N. Yang, (unpublished).

[72] J. Des Cloizeau and M. Gaudin, J. Math. Phys. **7**, 1384 (1966).

[73] D. L. Goodstein, *States of Matter*, (Dover Publications, New York, 1985).

[74] B. Sutherland, (to be published).

[75] R. A. Römer and B. Sutherland, submitted to Phys. Lett. A.

[76] D. Haldane, in *Proceedings of the 16th Taniguchi Symposium on the Theory of Condensed Matter: Correlation Effects in Low Dimensional Electron Systems*, N. Kawakami and A. Okiji (eds.), Springer Verlag (1994).

[77] E. R. Mucciolo, B. S. Shastry, B. D. Simons, and B. L. Altshuler, to appear in Phys. Rev. B.

[78] O. Narayan and B. S. Shastry, preprint.

[79] C. Itzykson, H. Saleur and J.B. Zuber, *Conformal Invariance and Applications to Statistical Mechanics*, (World Scientific, Hong Kong, 1988).

VITA

Rudolf Andreas Römer

Date of Birth:	February 22, 1966.
Place of Birth:	Gedern, Hessen (Germany).
Citizenship:	German.
Marital Status:	Married to Y. A. Wijesekara of Dondra, Sri Lanka.

Education:

Ph.D., 1994	Advisor: Prof. Bill Sutherland, University of Utah.
Diplom, 1991	Advisor: Prof. Robert Schrader, Freie Universität Berlin.
Abitur, 1985	Wolfgang-Ernst Gymnasium, Büdingen.

Employment:

TA (Level II), 1992/94	University Physics for Scientists and Engineers, University of Utah.
TA, 1992	College Physics for Scientists and Engineers, University of Utah.
Tutor, 1990/91	Physics for Physicists, Scientists and Engineers, Freie Universität Berlin.
TA, 1989/90	University Physics for Scientists and Engineers, Duke University, Durham.